Complementary Effects of In-Stream Structures and Inset Floodplains on Solute Retention

by

David L. Azinheira

Thesis submitted to the faculty of the Virginia Polytechnic Institute and State University in partial fulfillment of the requirements for the degree of

Master of Science
In
Civil Engineering

Erich T. Hester, Chair
W. Cully Hession
Durelle T. Scott IV
Mark A. Widdowson

April 30, 2013
Blacksburg, VA

Keywords: Hyporheic, Transient storage, Surface water-groundwater exchange, Pollutant attenuation, Stream restoration

Complementary Effects of In-Stream Structures and Inset Floodplains on Solute Retention

David L. Azinheira

Abstract

The pollution of streams and rivers is a growing concern, and environmental guidance increasingly suggests stream restoration to improve water quality. Solute retention in off-channel storage zones such as hyporheic zones and floodplains is typically necessary for significant reaction to occur. Yet the effects of two common restoration techniques, in-stream structures and inset floodplains, on solute retention have not been rigorously compared. We used MIKE SHE to model hydraulics and solute transport in the channel, inset floodplain, and hyporheic zone of a 2nd order stream. We varied hydraulic conditions (winter baseflow, summer baseflow, and storm flow), geology (hydraulic conductivity), and stream restoration design parameters (inset floodplain length, and presence of in-stream structures). In-stream structures induced hyporheic exchange during summer baseflow with a low groundwater table (~20% of the year), while floodplains only retained solutes during storm flow conditions (~1% of the year). Flow through the hyporheic zone increased linearly with hydraulic conductivity, while residence times decreased linearly. Flow through inset floodplains and residence times in both the channel and floodplains increased non-linearly with the fraction of bank with floodplains installed. The fraction of stream flow that entered inset floodplains was one to three orders of magnitude higher than that through the hyporheic zone, while the residence time and mass storage in the hyporheic zone was one to five orders of magnitude larger than that in floodplain segments. Our model results suggest that in-stream structures and inset floodplains are complementary practices.

Acknowledgements

I would like to thank everyone involved with the StREAM Lab (http://www.bse.vt.edu/site /streamlab/index.html), especially Cully Hession for helping me acquire stream gage, LIDAR, and longitudinal stream survey data for Stroubles Creek; Katie Brill for providing piezometer data for Stroubles Creek; Tess Thompson for supplying a restoration plan for Stroubles Creek; and Waverly Parks for pre-restoration survey data of Stroubles Creek. I thank the National Science Foundation for funding my work (views expressed here are those of the authors and not necessarily those of the NSF), and DHI for allowing me to use MIKE SHE for my thesis at no cost. I would also like to thank my family and friends for all of their support. Lastly, I would like to thank my advisor Erich Hester, as well as my committee members Cully Hession, Durelle Scott, and Mark Widdowson.

Table of Contents

List of Figures

List of Tables

List of Abbreviations

α	hyporheic hydraulic coefficient, m^2.
β	inset floodplain – main channel exchange coefficient, m^{-1}.
D_s	structure density, (# of structures)/m.
ε_t	transverse dispersion coefficient, m^2/s.
F_b	fraction of bank with inset floodplains, dimensionless.
K	hydraulic conductivity, m^2/s.
L_B	total length of bank, m.
L_{FP}	total length of inset floodplain, m.
L_R	length of reach where restoration has taken place, m.
M_{HZ}	mass of solute stored in the hyporheic zone, kg.[a]
M_{FP}	mass of solute stored in the inset floodplains, kg.[a]
M_{MC}	mass of solute stored in the main channel, kg.[a]
n	Manning's roughness coefficient, dimensionless.
$Q_{F\text{-}FP}$	fraction of surface water flow that enters inset floodplain, dimensionless.
$Q_{F\text{-}HZ}$	fraction of surface water flow that enters hyporheic zone, dimensionless
$Q_{GW\text{-}SW}$	flow from groundwater to surface water for a single grid cell, m^3/s.[a]
Q_{FP}	exchange flow between an inset floodplain grid cell and a main channel grid cell, m^3/s.[a]
$Q_{CHANNEL}$	total surface water flow through the main channel at the upstream boundary, m^3/s.[a]
RT_{FI}	fractional increase in the reach residence time due to storage zone, dimensionless.
StREAM Lab	Stream Research, Education, and Management Lab.
t_{50}	time to 50% of the breakthrough tracer curve steady state concentration, minutes.
t_{75}	time to 75% of the breakthrough tracer curve steady state concentration, minutes.
t_{99}	time to 99% of the breakthrough tracer curve steady state concentration, minutes.

[a]abbreviation only used in figures.

1. Introduction

1.1. Background

The health of streams and rivers in the United States has been degrading since the industrial revolution, with human impacts having an assortment of negative consequences [FISRWG, 1998]. For example, increasing impervious areas and the channelization of natural waterways is leading to higher channel velocities. Erosion due in part to higher channel velocities increases the loading of fine sediments, while shorter residence times limit pollutant attenuation. The application of fertilizers has further exacerbated this problem as nutrients (e.g., nitrogen and phosphorous) are added directly to lawns and agricultural fields, and often flow directly into streams and rivers with runoff [*Royer et al.*, 2006; *Walsh et al.*, 2005]. These nutrients along with fine sediment are currently the primary pollutants impacting streams in the United States [*Langland et al.*, 2000]. As a result of the prevalence of these impairments, stream restoration is a flourishing industry [*Bernhardt et al.*, 2005].

In practice the term "stream restoration" includes the processes associated with stream recovery, reestablishment, rehabilitation, and restoration [*Sawyer et al.*, 2011; *Sear*, 1994], and this is the terminology that will be used for this thesis. Stream restoration projects are often implemented in the United States as a result of stream mitigation (restoring a stream as a result of impacting another stream at a different location) [*BenDor et al.*, 2009], the Endangered Species Act [*Roni et al.*, 2002], and increasingly stringent regulations associated with Clean Water Act [*Copeland*, 2006]. The Clean Water Act has led to an increased focus on improving water quality in channels (e.g., reducing nitrate, phosphorous, and fine sediment) making it a common impetus for stream restoration projects [*Copeland*, 2006; *Schueler and Stack*, 2012]. There are various types of stream restoration practices and many of these are believed to improve water quality. These practices include channel realignment [*Mason et al.*, 2012], riparian planting [*Roni et al.*, 2002], installation of in-stream structures [*Hester and Gooseff*, 2010; *Radspinner et al.*, 2010], and floodplain reconnection [*Opperman et al.*, 2009].

For significant reaction of channel-borne pollutants to occur, all reactants must be present [*Schnoor*, 1996], there must be a sufficient residence time [*Schnoor*, 1996; *Zarnetske et al.*, 2011; *Zarnetske et al.*, 2012], and a sufficient proportion of stream flow must enter retention zones [*Wondzell*, 2011]. The maximum pollutant reaction potential of a system can then be assessed by analyzing solute retention (percent flow and residence time) and assuming all reactants are present. By analyzing the solute retention associated with different stream restoration practices the pollutant attenuation potential for individual stream restoration practices can be compared. The focus of this study will be on the solute retention associated with channel spanning in-stream structures and inset floodplains implemented in tandem for a stream in Virginia.

Inset floodplains (also known as in-channel benches, two-stage channels, berms, and incipient floodplains) are small floodplain benches at some elevation above the channel bed but below the standard bankfull floodplain [*Royall et al.*, 2010]. Inset floodplains are installed to decrease flow velocities during storms, often leading to a reduction in erosion [*Roley et al.*, 2012; *Thompson et al.*, 2012]. Floodplain sediment is well suited for reactions that attenuate pollutants, so water quality improvements are another potential benefit [*Noe and Hupp*, 2007; *Roley et al.*, 2012]. Channel spanning in-stream structures are common features of stream restoration projects, and include rock cross vanes [*Buchanan et al.*, 2012; *Daniluk et al.*, 2012; *Rosgen*, 2001], channel spanning wooden logs [*Sawyer and Cardenas*, 2012; *Sawyer et al.*, 2011], and steps [*Chin et al.*, 2009; *Endreny et al.*, 2011]. In-stream structures are typically installed for bed stabilization or habitat creation [FISRWG, 1998; *Rosgen*, 2001], but they also create drops in the water surface that induce hyporheic flow where short flowpaths leave and return to the surface stream [*Hester and Doyle*, 2008; *Lautz and Siegel*, 2006]. This in-stream structure induced hyporheic exchange augments the hyporheic exchange that occurs naturally in stream systems. Natural hyporheic exchange can occur at meander bends [*Boano et al.*, 2006], and pool-riffle sequences [*Storey et al.*, 2003].

Both in-stream structure induced hyporheic zones and inset floodplains may improve the ecological health of streams [*Hester and Gooseff*, 2010; *Roley et al.*, 2012]. In particular both can act as sinks of pollutants including nitrate [*Creswell et al.*, 2008; *Haycock and Burt*, 1993; *Noe and Hupp*, 2007; *Zarnetske et al.*, 2011] and phosphorous [*Heeren et al.*, 2011; *Noe and Hupp*, 2007]. By understanding and comparing the retention capabilities of each of these practices, their potential for improving water quality can be estimated. Studies like this are vital to better recognize how the various stream restoration practices retain solutes when installed in tandem, and will lead to a greater understanding of factors controlling water quality improvements.

1.2. Research Objectives

The objective of this study was to compare hyporheic solute retention induced by in-stream structures with surface solute retention induced by inset floodplains. Solute retention is an indicator of the water quality improvement potential for a stream. For this study we used numerical modeling of surface water and groundwater hydraulics and coupled solute tracer transport using MIKE SHE for a 90 m reach of Stroubles Creek in Blacksburg, Virginia. A model was created for Stroubles Creek and the geology (hydraulic conductivity), hydraulics (groundwater levels and stream stage) and restoration design (inset floodplain length and presence of in-stream structures) were varied. ~~The r~~Retention metrics (i.e. flow, mass storage, and residence times) were analyzed for each model scenario. Our specific objectives

were to determine how inset floodplain induced surface solute retention and in-stream structure induced hyporheic solute retention differed in terms of:

(1) When during the year they were active;

(2) The proportion of stream flow expected to travel through them when active;

(3) Their residence times (and corresponding effect on reach residence time); and

(4) The total mass of solute stored.

1.3. Organization of Thesis

This document is organized around a journal article that will be submitted for publication in *Water Resources Research*. This article is located in Section 2 of this thesis and is the central component of this study. Section 3 is a summary of the engineering significance of this study, and it is followed by supporting material with a more detailed description of modeling methodology used for this study.

Section 2

Azinheira, D.L., D.T. Scott, and E.T. Hester (2013), Complementary effects of in stream structures and inset floodplains on solute retention. To be submitted to *Water Resources Research*.

1.4. References

BenDor, T., J. Sholtes, and M. W. Doyle (2009), Landscape characteristics of a stream and wetland mitigation banking program, *Ecological applications*, *19*(8), 2078-2092.

Bernhardt, E. S., et al. (2005), Synthesizing U.S. river restoration efforts, *Science*, *308*(5722), 636-637.

Boano, F., C. Camporeale, R. Revelli, and L. Ridolfi (2006), Sinuosity-driven hyporheic exchange in meandering rivers, *Geophysical Research Letters*, *33*(18).

Buchanan, B., M. Walter, G. Nagle, and R. Schneider (2012), Monitoring and assessment of a river restoration project in central New York, *River Research and Applications*, *28*(2), 216-233.

Chin, A., S. Anderson, A. Collison, B. J. Ellis-Sugai, J. P. Haltiner, J. B. Hogervorst, G. M. Kondolf, L. S. O'Hirok, A. H. Purcell, and A. L. Riley (2009), Linking theory and practice for restoration of step-pool streams, *Environmental Management*, *43*(4), 645-661.

Copeland, C. (2006), Water Quality: Implementing the Clean Water Act *Rep.*, Congressional Research Service Reports. Paper 36.

Creswell, J. E., S. C. Kerr, M. H. Meyer, C. L. Babiarz, M. M. Shafer, D. E. Armstrong, and E. E. Roden (2008), Factors controlling temporal and spatial distribution of total mercury and methylmercury in hyporheic sediments of the Allequash Creek wetland, northern Wisconsin, *Journal of Geophysical Research: Biogeosciences*, *113*(G2), G00C02, doi: 10.1029/2008JG000742.

Daniluk, T. L., L. K. Lautz, R. P. Gordon, and T. A. Endreny (2012), Surface water–groundwater interaction at restored streams and associated reference reaches, *Hydrological Processes*, doi: 10.1002/hyp.9501.

Endreny, T., L. Lautz, and D. Siegel (2011), Hyporheic flow path response to hydraulic jumps at river steps: Flume and hydrodynamic models, *Water Resources Research*, *47*(2), W02517, doi: 10.1029/2009WR008631.

FISRWG (Federal Interagency Stream Restoration Working Group) (1998), Stream corridor restoration : principles, processes, and practices *Rep. 0934213593 9780934213592*, Federal Interagency Stream Restoration Working Group, Washington, D.C.

Haycock, N. E., and T. P. Burt (1993), Role of floodplain sediments in reducing the nitrate concentration of subsurface run-off: A case study in the Cotswolds, UK, *Hydrological Processes*, *7*(3), 287-295, doi: 10.1002/hyp.3360070306.

Heeren, D. M., G. A. Fox, R. B. Miller, D. E. Storm, A. K. Fox, C. J. Penn, T. Halihan, and A. R. Mittelstet (2011), Stage-dependent transient storage of phosphorus in alluvial floodplains, *Hydrological Processes*, *25*(20), 3230-3243, doi: 10.1002/hyp.8054.

Hester, E. T., and M. W. Doyle (2008), In-stream geomorphic structures as drivers of hyporheic exchange, *Water Resources Research*, *44*(3), W03417, doi: 10.1029/2006WR005810.

Hester, E. T., and M. N. Gooseff (2010), Moving beyond the banks: hyporheic restoration is fundamental to restoring ecological services and functions of streams, *Environmental Science & Technology*, *44*(5), 1521-1525.

Langland, M. J., J. D. Blomquist, L. A. Sprague, and R. E. Edwards (2000), *Trends and status of flow, nutrients, and sediments for selected nontidal sites in the Chesapeake Bay Watershed, 1985-98*, US Department of the Interior, US Geological Survey.

Lautz, L. K., and D. l. Siegel (2006), Modeling surface and ground water mixing in the hyporheic zone using MODFLOW and MT3D, *Advances in Water Resources*, *29*(11), 1618-1633.

Mason, S. J. K., B. L. McGlynn, and G. C. Poole (2012), Hydrologic response to channel reconfiguration on Silver Bow Creek, Montana, *Journal of Hydrology (Amsterdam)*, *438*(1), 125-136.

Noe, G. B., and C. R. Hupp (2007), Seasonal variation in nutrient retention during inundation of a short-hydroperiod floodplain, *River Research and Applications*, *23*(10), 1088-1101.

Opperman, J. J., G. E. Galloway, J. Fargione, J. F. Mount, B. D. Richter, and S. Secchi (2009), Sustainable floodplains through large-scale reconnection to rivers, *Science*, *326*(5959), 1487-1488.

Radspinner, R., P. Diplas, A. F. Lightbody, and F. Sotiropoulos (2010), River training and ecological enhancement potential using in-stream structures, *Journal of Hydraulic Engineering*, *136*(12), 967-980.

Roley, S. S., J. L. Tank, and M. A. Williams (2012), Hydrologic connectivity increases denitrification in the hyporheic zone and restored floodplains of an agricultural stream, *Journal of Geophysical Research*, *117*, G00N04, doi: 10.1029/2012JG001950.

Roni, P., T. J. Beechie, R. E. Bilby, F. E. Leonetti, M. M. Pollock, and G. R. Pess (2002), A review of stream restoration techniques and a hierarchical strategy for prioritizing restoration in pacific northwest watersheds, *North American Journal of Fisheries Management*, *22*(1), 1-20.

Rosgen, D. L. (2001), The Cross-Vane, W-Weir and J-Hook Vane Structures...Their Description, Design and Application for Stream Stabilization and River Restoration, in *Wetlands Engineering & River Restoration 2001*, edited, pp. 1-22, American Society of Civil Engineers.

Royall, D., L. Davis, and D. R. Kimbrow (2010), In-channel benches in small watersheds: examples from the southern piedmont, *Southeastern Geographer*, *50*(4), 445-467.

Royer, T. V., M. B. David, and L. E. Gentry (2006), Timing of riverine export of nitrate and phosphorus from agricultural watersheds in illinois: implications for reducing nutrient loading to the Mississippi River, *Environmental Science & Technology*, *40*(13), 4126-4131.

Sawyer, A. H., and M. B. Cardenas (2012), Effect of experimental wood addition on hyporheic exchange and thermal dynamics in a losing meadow stream, *Water Resources Research*, *48*(10), W10537, doi: 10.1029/2011WR011776.

Sawyer, A. H., M. B. Cardenas, and J. Buttles (2011), Hyporheic exchange due to channel-spanning logs, *Water Resources Research*, *47*(8), W08502, doi: 10.1029/2011WR010484.

Schnoor, J. L. (1996), *Environmental Modeling: Fate and Transport of Pollutants in Water, Air, and Soil*, John Wiley and Sons.

Schueler, T., and B. Stack (2012), Recommendations of the Expert Panel to Define Removal Rates for Individual Stream Restoration Projects: Final Report *Rep.*, Chesapeak Bay Urban Stormwater Workgroup.

Sear, D. A. (1994), River restoration and geomorphology, *Aquatic Conservation: Marine and Freshwater Ecosystems*, *4*(2), 169-177.

Storey, R. G., K. W. F. Howard, and D. D. Williams (2003), Factors controlling riffle-scale hyporheic exchange flows and their seasonal changes in a gaining stream: A three-dimensional groundwater flow model, *Water Resources Research*, *39*(2), n/a-n/a, doi: 10.1029/2002WR001367.

Thompson, W., C. W. Hession, and D. T. Scott (2012), StREAM Lab at Virginia Tech, *Resources*, *19*(2), 8-9.

Walsh, C. J., A. H. Roy, J. W. Feminella, P. D. Cottingham, P. M. Groffman, and R. P. Morgan II (2005), The urban stream syndrome: current knowledge and the search for a cure, *Journal of the North American Benthological Society*, *24*(3), 706-723.

Wondzell, S. M. (2011), The role of the hyporheic zone across stream networks, *Hydrological Processes, 25*(22), 3525-3532, doi: 10.1002/hyp.8119.

Zarnetske, J. P., R. Haggerty, S. M. Wondzell, and M. A. Baker (2011), Dynamics of nitrate production and removal as a function of residence time in the hyporheic zone, *Journal of Geophysical Research, 116*(G1), G01025.

Zarnetske, J. P., R. Haggerty, S. M. Wondzell, V. A. Bokil, and R. González-Pinzón (2012), Coupled transport and reaction kinetics control the nitrate source-sink function of hyporheic zones, *Water Resources Research, 48*(11), W11508, doi: 10.1029/2012WR011894.

2. Complementary Effects of In-Stream Structures and Inset Floodplains on Solute Retention

2.1. Introduction

2.1.1. Stream Restoration Goals and Techniques

The degradation of streams and rivers in the United States is well documented [FISRWG, 1998], and stream restoration is a flourishing industry [*Bernhardt et al.*, 2005]. Typical objectives of restoration include improving bank stability [*Buchanan et al.*, 2012], aesthetics [*Kondolf and Micheli*, 1995], habitat creation [*Box*, 1996; *Roni et al.*, 2002], and water quality [*Craig et al.*, 2008; *Filoso and Palmer*, 2011]. Stream restoration projects are often implemented to mitigate impacts elsewhere [*BenDor et al.*, 2009], to create habitat under the Endangered Species Act [*Roni et al.*, 2002], and increasingly to improve water quality under the Clean Water Act ~~[*Copeland*, 2006]~~[*Copeland*, 2006; *Schueler and Stack*, 2012]. Stream restoration strategies such as channel realignment [*Mason et al.*, 2012], riparian planting [*Roni et al.*, 2002], installation of in-stream structures [*Hester and Gooseff*, 2010; *Radspinner et al.*, 2010], and floodplain reconnection [*Opperman et al.*, 2009] help meet multiple restoration objectives (including improving water quality), although they are often installed with a single objective in mind.

Channel spanning in-stream structures are a common feature of stream restoration projects, and include rock cross vanes [*Rosgen*, 2001; *Buchanan et al.*, 2012; *Daniluk et al.*, 2012], channel-spanning logs [*Sawyer et al.*, 2011; *Sawyer and Cardenas*, 2012], and steps [*Chin et al.*, 2009; *Endreny et al.*, 2011a]. In-stream structures are typically installed for bed stabilization or habitat creation [FISRWG, 1998; *Rosgen*, 2001], but they also create drops in the water surface which induce hyporheic flow where short flowpaths leave and return to the surface stream [*Wondzell and Swanson*, 1996; *Lautz and Siegel*, 2006; *Hester and Doyle*, 2008; *Wondzell*, 2011; *Ward et al.*, 2012] . Such structure induced "hyporheic flow cells" augment similar exchange zones that occur naturally due to meander bends [*Boano et al.*, 2006], ~~and~~ pool-riffle sequences [*Storey et al.*, 2003], ~~as well as~~and turbulence in coarse substrate [*Nagaoka and Ohgaki*, 1990]. Such hyporheic zones create benthic or hyporheic habitat, cycle nutrients, attenuate pollutants, and moderate temperature; all of which can improve the ecological health of a stream [*Brunke and Gonser*, 1997]. Potential water quality improvements (e.g., denitrification) due to hyporheic flow are of particular interest for this study, though the hyporheic zone can act as either a source or a sink of pollutants [*Creswell et al.*, 2008; *Zarnetske et al.*, 2011].

Inset floodplains (also known as in-channel benches, two-stage channels, berms, and incipient floodplains) are small floodplain benches at some elevation above the channel bed but below the standard bankfull floodplain [*Royall et al.*, 2010]. Inset floodplains form naturally when streams are recovering from extreme bank erosion linked to high flood frequencies [*Royall et al.*, 2010], and have been found to retain organic material [*Changxing et al.*, 1999; *Thoms and Olley*, 2004]. Unlike bankfull floodplains that are typically inundated annually or biannually [*Soar and Thorne*, 2011], inset floodplains are inundated

several times during the course of the year. Bankfull floodplains act as either sources or sinks of pollutants (e.g., excess nitrate and phosphorous) for short duration floods [*Haycock and Burt*, 1993; *Noe and Hupp*, 2007; *Heeren et al.*, 2011]. Since inset floodplains are also typically inundated for short durations, similar processes are expected. Relatively few studies have investigated pollutant removal due specifically to inset floodplains, although inset floodplains can increase denitrification potential in streams [*Roley et al.*, 2012b; *Roley et al.*, 2012a].

2.1.2. Effects of Multiple Techniques on Solute Retention and Water Quality

A few studies have observed the effects of complementary stream restoration practices, including the effects of riparian vegetation and baffles [*Ensign and Doyle*, 2005], and the effects of adding stream features (e.g. pools and riffles) and relocating a channel to its floodplain [*Bukaveckas*, 2007]. Other studies have observed how specific restoration design choices coupled with various environmental factors affect solute retention in the hyporheic zone [*Hester and Doyle*, 2008; *Sawyer et al.*, 2011] or inset floodplains [*Roley et al.*, 2012a]. Yet the complementary nature of in-stream structures and inset floodplains has not been analyzed to our knowledge.

For significant reaction of channel-borne pollutants to occur, all reactants must be present [*Schnoor*, 1996], there must be a sufficient residence time [*Schnoor*, 1996; *Zarnetske et al.*, 2011; *Zarnetske et al.*, 2012], and a sufficient proportion of stream flow must enter the retention zone (percent flow) [*Wondzell*, 2011]. The maximum pollutant reaction potential of a system can be assessed by analyzing solute retention (percent flow and residence time) and assuming all reactants are present. Pollution attenuation (e.g., denitrification) in river networks is typically concentrated in small streams [*Alexander et al.*, 2000]. The fraction of stream flow entering the hyporheic zone is typically expected to be low [*Wondzell*, 2011], although residence times are generally sufficient for reactions to occur [*Zarnetske et al.*, 2011; *Zarnetske et al.*, 2012]. Neither the fraction of channel water traveling through inset floodplains, nor inset floodplain residence times have been analyzed previously.

Pollution of waterways from nutrient loading is a major concern in the United States [*Cerco and Cole*, 1993; *Rabalais et al.*, 2002]. Excess nitrogen is considered one of the great engineering challenges of the twenty-first century [*Vest*, 2008]. A significant portion of pollutants travel downstream during storm flows [*Owens et al.*, 1991; *Royer et al.*, 2006], with some (e.g., phosphorous and fine sediment) moving downstream principally during storm flow, while others (e.g. nitrate) are transported more evenly between storm and non-storm events [*Pionke et al.*, 1999]. Stream restoration techniques will vary in their effects among these different flow regimes. Inset floodplains by definition are only activated during storms, and are disengaged during most of the year. They have potential for removing nitrate (via denitrification) during storms [*Roley et al.*, 2012b; *Roley et al.*, 2012a], although they can also be net

sources of nitrate [*Noe and Hupp*, 2007]. By contrast, in-stream structures lead to solute retention primarily during baseflow [*Wondzell and Swanson*, 1996; *Ward et al.*, 2012] by inducing hyporheic flow cells and in-channel backwater storage [*Ensign and Doyle*, 2005; *Hester and Doyle*, 2008]. Hyporheic zones have been much discussed for their promise of water quality benefits [*Hester and Gooseff*, 2010], and have been shown to be effective at attenuating pollutants during baseflow [*Kim et al.*, 1995]. In-stream structures and inset floodplains may therefore complement each other in regards to when they are important (i.e. baseflow or storm flow), and what reaction condition they maximize (e.g., residence time or percent of stream flow entering retention zone).

2.1.3. Objectives of Study

The aim of this study was to compare hyporheic solute retention induced by in-stream structures with surface solute retention within inset floodplains. We numerically modeled surface water and groundwater hydraulics and coupled conservative tracer transport in a 90 m reach of Stroubles Creek in Blacksburg, Virginia. Our specific objectives were to determine how inset floodplain and in-stream structure induced solute retention differ in terms of: (1) when during the year they are active; (2) the proportion of stream flow expected to travel through them when active; (3) their residence times (and corresponding effect on reach residence time); and (4) the total mass of solute stored. We analyzed these retention metrics while varying the restoration design parameters (e.g., inset floodplain length), geology, and hydraulic conditions.

2.2. Methods

2.2.1. Model Selection and Governing Equations

We used MIKE SHE, a finite difference integrated hydraulic model with coupled three-dimensional groundwater and two-dimensional surface water [*Graham and Butts*, 2005; DHI, 2011]. The groundwater component of MIKE SHE uses the groundwater flow equation:

$$\frac{\partial}{\partial x}\left(K_{xx}\frac{\partial h}{\partial x}\right)+\frac{\partial}{\partial y}\left(K_{yy}\frac{\partial h}{\partial y}\right)+\frac{\partial}{\partial z}\left(K_{zz}\frac{\partial h}{\partial z}\right)-Q=S\frac{\partial h}{\partial t} \qquad (1)$$

where K_{xx} is the hydraulic conductivity in the *x* direction (m/s), K_{yy} is the hydraulic conductivity in the y direction (m/s), K_{zz} is the hydraulic conductivity in the *z* direction (m/s), h is the hydraulic head, Q is the source/sink term (m^3/s), and S is the storage coefficient (m^{-1}) [DHI, 2011]. MIKE SHE uses a fully implicit three-dimensional finite difference algorithm to solve the groundwater flow equation [*Graham and Butts*, 2005]. The surface water component of MIKE SHE uses the two-dimensional diffusive wave

approximation of the Saint Venant equation solved using an explicit algorithm [*Graham and Butts*, 2005]. The Saint Venant Equation in the downstream direction is:

$$\underset{(i)}{\frac{\partial u}{\partial t}} + \underset{(ii)}{u\frac{\partial u}{\partial x}} + \underset{(iii)}{g\frac{\partial h}{\partial x}} + \underset{(iv)\ (v)}{g(S_f - S_0)} = 0 \qquad (2)$$

where x is the distance in the downstream direction (m), u is the velocity component in the x direction (m/s), t is time (s), g is gravity (m/s^2), h is the depth of water (m), S_f is the slope of the energy grade line (dimensionless), and S_0 is the channel slope (dimensionless) [*Moussa and Bocquillon*, 2000; *Tsai*, 2005]. The terms above describe (*i*) local acceleration, (*ii*) convective acceleration, (*iii*) pressure gradient, (*iv*) friction, and (*v*) gravity. For the transverse direction Equation (2) is written in terms of y (the distance in the transverse direction) and v **(**the velocity in the y direction) instead of x and u respectively [DHI, 2011].

The diffusive wave assumes that the local acceleration (*i*) and the convective acceleration (*ii*) can be disregarded, which is reasonable since the pressure gradient (*iii*) and the slope (*v*) are generally an order of magnitude larger than these terms [*Henderson*, 1966]. In this study hydraulics were run to steady state so the local acceleration (*i*) is zero and only the convective acceleration (*ii*) is omitted. Generally, simplifications of Saint Venant equation lead to similar results to the full equation but take less time to run [*Horritt and Bates*, 2001]. The diffusive wave simplification has been used successfully in various studies where overbank flooding occurs [*Hromadka et al.*, 1985; *Giammarco et al.*, 1996; *Weill et al.*, 2009].

2.2.2. Model Setup

2.2.2.1. Study Site

The study site is a 90 m long reach of a 1.5 km restored segment of Stroubles Creek, a 2nd order stream in Blacksburg Virginia. The site is within the Stream Research, Education, and Management Lab (StREAM Lab, http://www.bse.vt.edu/site /streamlab/index.html) that has been monitored by the Virginia Tech Biological Systems Engineering Department since 2008 [*Thompson et al.*, 2012]. The drainage area of the reach is approximately 15 km^2, with primarily urban and agricultural land use. Prior to restoration completion in 2010, inset floodplains were forming naturally at several meanders. As a result, inset floodplains were incorporated into the restoration design along with riparian zone planting and bank stabilization. Vegetation ranges from grasses to brush on the inset floodplains. Vegetation is primarily grasses on the bankfull floodplain along with saplings planted during the restoration. The inset floodplains were originally designed to contain the 2.5 year flood while not mobilizing sediment larger

than the 84th quantile of the bed grain size distribution [*Resop*, 2010]. There are currently no in-stream structures present. We chose this location for our modeling study because (1) the drainage area was both urban and agricultural and was therefore a typical candidate for restoration [FISRWG, 1998], (2) both natural and constructed inset floodplains were present, (3) hydrologic data was available for model development, and (4) if research results were favorable in-stream structures could be installed in the future.

2.2.2.2. Model Domain and Computational Grid

We determined the location and extent of the model domain ~~were~~ based on the geometry of Stroubles Creek and the availability of groundwater data. Restoration of 1.5 km of Stroubles was completed in early 2010; however, inset floodplains were only installed along a 500 m reach [*Wynn et al.*, 2010]. Within this reach there is a transect of 6 piezometer nests oriented perpendicularly to the channel with 3 nests extending east and 3 extending west. We used water level data from the 4 piezometer nests closest to the streams to represent the groundwater conditions adjacent to the stream (Figure 1). Each nest is composed of a shallow and a deep piezometer, although only the deep piezometers were used for this study because the water table was often below the shallow piezometers. There are intermittent water table data from this transect from 2010 to 2012, as well as approximately one year of continuous data in 2010. The model domain extended laterally (perpendicularly to the channel) out to the 2nd piezometer nest away from the channel resulting in a model width of 75 ~~m.~~ m. This allowed hydraulic data from these piezometers to be used as boundary conditions. The longitudinal model domain length (100 m) was chosen to include a sufficient number of meanders for analysis of inset floodplains (four). The grid discretization (1 m by 1 m) was selected as a compromise between model run time and a grid resolution fine enough to adequately simulate structure-induced hyporheic flow and produce a relatively smooth channel bed. The horizontal pattern of groundwater and surface water grids in MIKE SHE must be identical [DHI, 2011] so both the surface water and groundwater grid were 1 m^2 in the horizontal direction. With this grid resolution there were 102 rows, 77 columns, and 7,850 cells.

The groundwater layer thickness was held constant vertically (i.e., at a given horizontal location), but varied when moving from one cell to another laterally or longitudinally. The groundwater layer thickness below the thalweg was set to 0.2 m. The lower extent of the groundwater domain (5 m below the thalweg) was selected so hyporheic flow was not affected by the no-flow boundary at the bottom of the model domain. The number of vertical layers (25) was held constant horizontally throughout the model domain such that the layers were thicker beneath the bankfull floodplain than beneath the channel.

2.2.2.3. Topography and Bathymetry, Including Inset Floodplains

We derived surface topography from stream cross sections surveyed in 2012 superimposed over a LIDAR elevation grid from 2009 (pre-restoration). The points were converted to a raster in ArcGIS, then imported and interpolated into a 1 m by 1 m MIKE elevation grid file. Inset floodplains were surveyed at the restored reach of Stroubles Creek during the summer of 2012 using a Johnson Level & Tool electronic self-leveling horizontal rotary laser level (40-6535). Seven transects were surveyed at approximately 50 m intervals down the channel, with elevations measured at a maximum of 2 m horizontal intervals along the transects. The thalweg as well as the edges of bankfull floodplains, inset floodplains, and the channel were also surveyed at each transect.

To help generalize our results, we created a simplified channel-floodplain cross section by taking the averages of key geometric parameters from the 7 surveyed cross sections (Figure 2). The average longitudinal channel slope of 0.0023 m/m was calculated from a 2011 StREAM lab survey, and a pre-restoration "incised" bank slope was estimated from a 2009 StREAM lab stream survey. The incised bank slope was used for cross sections where inset floodplains were not present. We estimated the apex of the four primary meanders, and the inset floodplain segments were centered at these locations. Elevation grids were created such that the inset floodplain length at each meander was 0, 10, 20, and 30 meters long (centered at the meander apex,) (Figure 1). We also created a full inset floodplain scenario that extended as far as the most downstream and upstream segments of the 30 m inset floodplains on both banks without any breaks (the length for this scenario is 90 m). These inset floodplain lengths were specific to Stroubles Creek so we generalized the length by calculating

$$F_b = \frac{L_{FP}}{L_B} \qquad (3)$$

where F_b is the fraction of bank with inset floodplain, L_{FP} is the total length of inset floodplain added (m), and L_B is the total length of stream bank (m). The 5 different floodplain scenarios discussed above correspond with a F_b of 0.00, 0.22, 0.44, 0.67, and 1.0, respectively. We superimposed the simplified cross sections over the LIDAR grid creating grid files with the existing LIDAR derived topography overlaid with the interpolated channel for each of the inset floodplain scenarios.

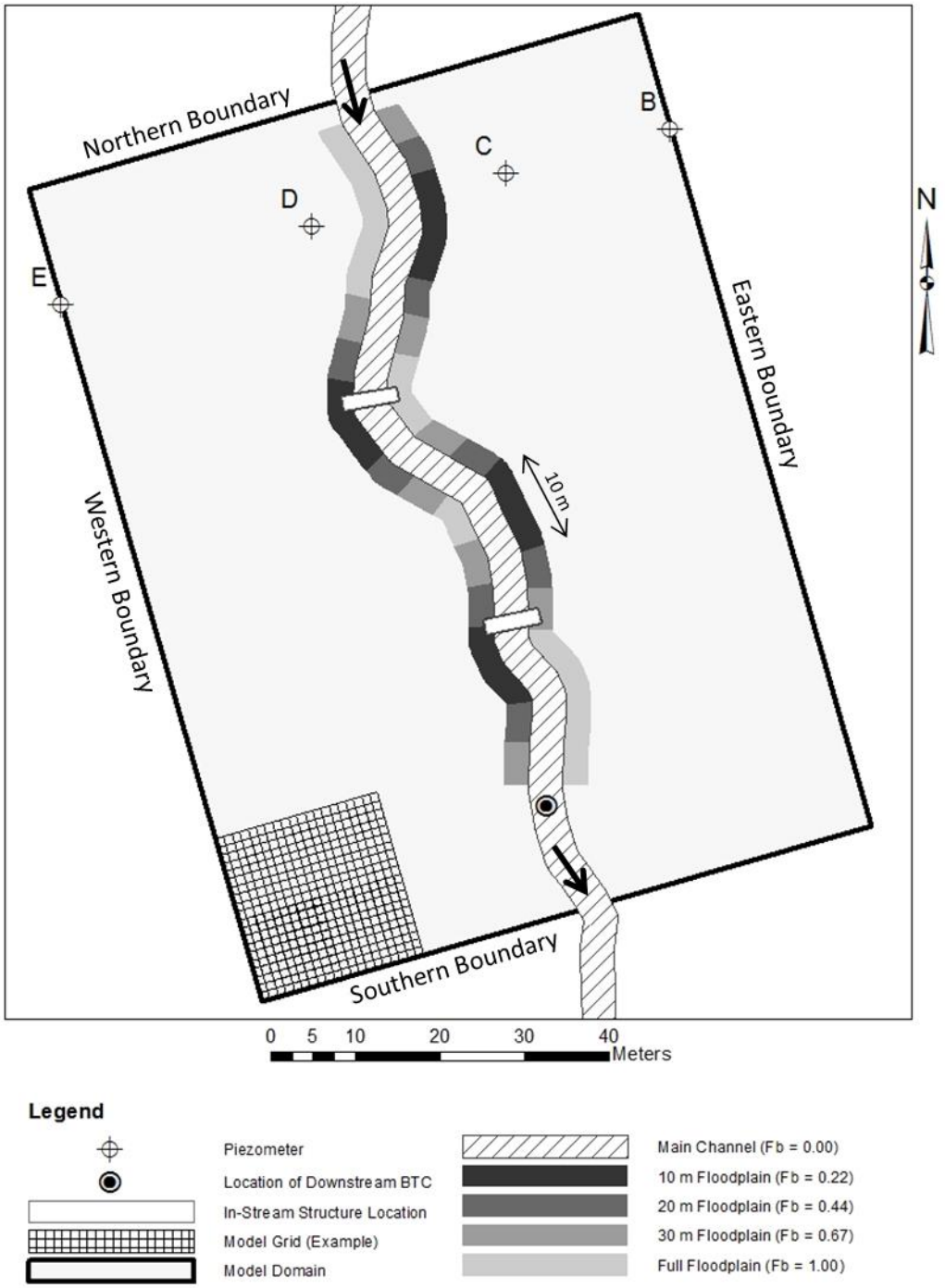

Figure 1. Inset floodplain location and extent for all floodplain scenarios modeled. Floodplain scenarios are defined by their length of individual inset floodplains and fraction of bank with floodplains (F_b). The model grid is displayed for a portion of the model domain, and the location where the breakthrough tracer curve (BTC) is taken downstream of the floodplain is also shown (see Results). Arrows indicate direction of stream flow.

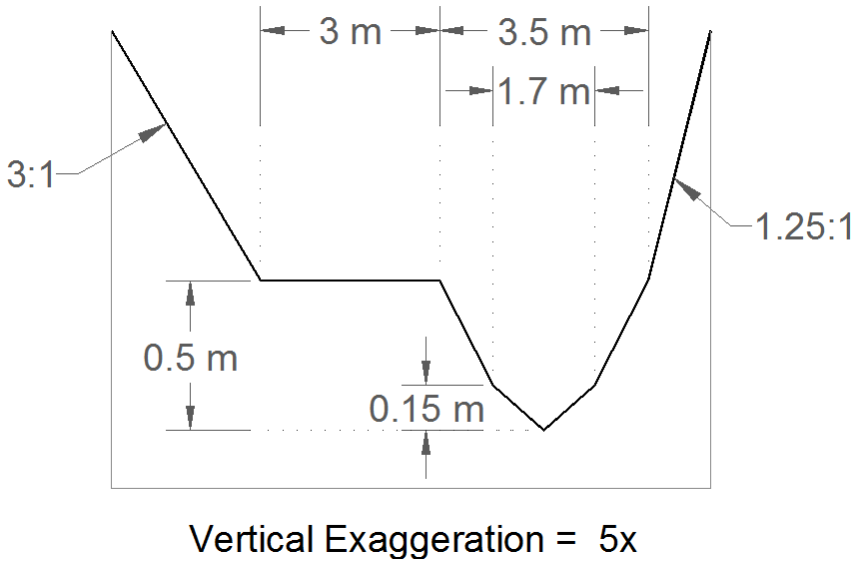

Figure 2. Simplified channel and floodplain cross section geometry used for modeling with restored inset floodplain (left bank), and pre-restoration incised bank (right bank). We used four variations of this cross section: incised channel on both banks, inset floodplain on the left bank only (shown), inset floodplain on the right bank only, and inset floodplain on both banks.

2.2.2.4. Surface Water Properties

There are three physical inputs for modeling surface water hydraulics and solute transport in MIKE SHE: Manning's roughness coefficient (n), the transverse dispersion coefficient (ε_t), and the longitudinal dispersion coefficient [DHI, 2011]. We estimated n using the methods outlined by *McCuen* [2005] for the main channel and from *Arcement et al.* [1989] for the inset floodplain. Both methods are based on channel and floodplain properties (i.e. regularity of channel, flow obstructions, variation of x-sections, vegetation, and degree of meandering). GIS was used to calculate the sinuosity while a field inspection was used to estimate the remaining parameters. The channel n used for modeling was 0.03 and the inset floodplain n during the summer was 0.07. We conducted a sensitivity analysis to confirm that varying n from our assumed values did not affect our conclusions (see Discussion).

We estimated ε_t in the field using the method outlined by *Fischer* [1979] for side discharge of a conservative visual tracer (i.e. suspended silt particles) using

$$L = \frac{0.4\bar{u}W^2}{\varepsilon_t} \qquad (4)$$

where L is the mixing length (m), ū is the average stream velocity (m/s), W is the channel width (m), and ε_t is the dispersion coefficient in the transverse direction (m^2/s). We estimated the mixing length at 14

~~m,~~ m, corresponding to an ε_t of 0.04 m^2/s, consistent with other field studies [*Fischer*, 1973; *Fischer et al.*, 1979]. We conducted a sensitivity analysis to confirm that varying ε_t from our assumed values did not significantly affect our conclusions (see Discussion). When considering longitudinal mixing, the effects of advection and longitudinal dispersion are additive [*Fischer et al.*, 1979]. Since advective mixing is approximately 40 times larger than longitudinal dispersion [*Fischer et al.*, 1979], a longitudinal dispersion coefficient of 0 ~~is~~ was used.

2.2.2.5. Soil/Sediment Properties

We used two porous media textures in the model: clay loam (bank and floodplain soil) and silty-gravel (stream bed and aquifer**,** Figure 3). We selected values for hydraulic conductivity (K) from StREAM Lab field slug tests performed in the summer of 2009 and from accepted literature values [*Holtz and Kovacs*, 1981; *Anderson and Woessner*, 1992] (Table 1). The base case stream sediment and aquifer K used for the study was 1×10^{-6} m/s. We used accepted values from the literature for porosity, specific yield, and specific storage [*Freeze and Cherry*, 1979; *Holtz and Kovacs*, 1981; *Anderson and Woessner*, 1992]. Groundwater hydrodynamic dispersivities were set to representative values for local dispersivity from the literature [*Gelhar et al.*, 1992; *Cirpka et al.*, 1999; *Cirpka and Kitanidis*, 2000; *Sawyer and Cardenas*, 2012] (Table 1). The location of the two soils was based on StREAM Lab soil borings, and cells that included both soil types used a weighted average to calculate hydraulic properties. We varied the K of the stream bed and aquifer from a silty-clay (1×10^{-8} m/s) to a coarse sand (1×10^{-4} m/s) [*Holtz and Kovacs*, 1981; *Anderson and Woessner*, 1992]. This represented urban and agricultural streams where fine sediments are prevalent [*Wood and Armitage*, 1997; *Calver*, 2005]. We assumed the stream bed was homogeneous and isotropic, but acknowledge that soil in natural systems is typically heterogeneous with preferential flow [*Cardenas et al.*, 2004], including flow through macropores [*Menichino et al.*, 2012]. We did not vary the K of the bank and floodplain soil.

Table 1. Summary of base case soil property values used for hydraulic and solute transport modeling

Description	Bank and Floodplain	Stream Bed and Aquifer
Soil Type	Clay Loam	Silty-Gravel
Hydraulic Conductivity (K), m/s	1×10^{-8}	1×10^{-6}
Porosity	0.49	0.30
Specific Storage, 1/m	0.001	0.0005
Specific Yield	0.13	0.20
Longitudinal Dispersivity, m	0.01	0.01
Transverse Dispersivity, m	0.001	0.001

2.2.2.6. Boundary Conditions

For the groundwater portion of the model domain, we used a no flow boundary at the lower extent of the domain, and fixed head boundaries along the northern, southern, eastern, and western boundaries (Figure 1). We used two sets of groundwater fixed head boundary conditions for this study, a summer steady state condition and a winter steady state condition. Both conditions were estimated from StREAM Lab piezometer data from 2009 to 2012 (Table 2). During the summer of 2009 an additional piezometer transect was monitored 120 m downstream of the transect used for this study with approximately the same orientation and spacing. There was variation in the groundwater depth below the ground surface from one transect to the next for the inner piezometers (i.e. piezometers C and D in Figure 1) of up to 1.3 ~~m,~~ m, while the variation in depth below the ground surface for the outer piezometers (i.e. piezometers B and E in Figure 1) was less than 0.4 m during the period of record. As a result, for the eastern and western boundaries we assumed the water table was located at a constant depth below the ground surface. We used the depths measured at piezometers B and E, respectively, and varied the groundwater table elevation based on the topography. For the northern fixed head boundary we used the depth below ground surface for piezometers B, C, D, and E as well as the stream level and linearly interpolated. For the southern boundary we only used the depth below ground surface indicated by the outer piezometers (i.e. B and E) and the stream level to interpolate the groundwater boundary conditions.

Table 2. Approximate average steady state summer and winter groundwater depths for active piezometers

Piezometer	Depth of phreatic surface below ground surface, m	
	Winter	Summer
B	0	1
C	0	1.2
D	0.5	1.4
E	0.2	1.3

The surface water flow component of the model required specified stages at the upstream and downstream boundaries. A StREAM Lab stream gage is located 300 m upstream of the study site without any significant tributaries in between. Three steady state stages were estimated using continuous data collected at this gage from May 2011 to May 2012: summer baseflow (depth of 0.1 m), winter baseflow (depth of 0.15 m) and storm flow (depth of 0.65 m). For the storm stage we selected the median of all inset floodplain activating stages (depth > 0.5 m) over the course of the gaging period. The existing site is closest to the scenario with inset floodplain lengths of 20 m ($F_b = 0.44$) with no in-stream structures, so we used this case to calculate channel discharge by inputting each of the three steady state stages as boundary conditions. Using this method we found that the stream flows for summer baseflow, winter baseflow, and storm flow were 0.025 m^3/s, 0.059 m^3/s, and 1.7 m^3/s respectively. These flows were held constant for all additional model runs by adjusting the surface water boundary conditions.

We combined these surface water boundary conditions with the groundwater boundary conditions to produce three sets of overall hydraulic boundary conditions (Figure 3). These scenarios were (1) a summer baseflow scenario (summer baseflow with summer steady state groundwater), (2) a winter baseflow scenario (winter baseflow with winter steady state groundwater), and (3) a storm flow scenario (storm flow with summer steady state groundwater). Although unsaturated (vadose) zone processes were not modeled, during storm flow scenarios channel water flowed into the inset floodplains which were situated over the unsaturated zone (Figure 3). In these situations MIKE-SHE uses Darcy's law to calculate the flow of recharge from surface water to the saturated zone. However, since the floodplain sediment is fine ($K = 1\times10^{-8}$ m/s) this recharge had a negligible effect on the saturated zone over a storm duration. Hydraulic model mass balance errors were less than 0.2% for all model runs.

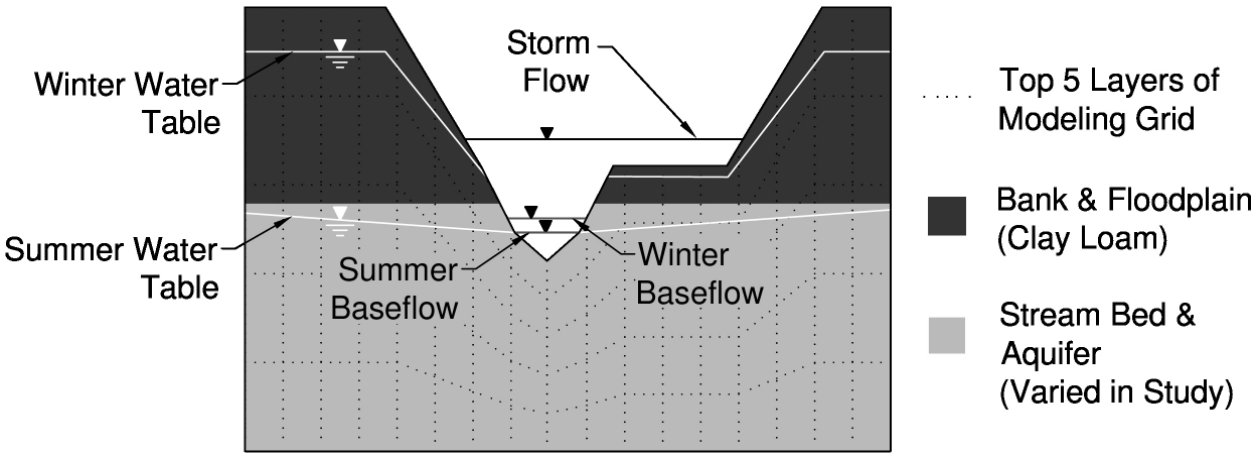

Figure 3. Conceptual diagram of hydrological conditions and soil/sediment texture used in model with 5 upper model layers shown. When multiple soil/sediment textures are present in a single cell a weighted average is calculated for all hydraulic properties.

For solute transport we input a conservative tracer at the upstream surface water boundary (northern model boundary) with a constant concentration of 1 g/m^3 (Figure 1). We used a step tracer increase for all solute tracer analyses, and turned the tracer loading off after 10 minutes for storm flow scenarios to better visualize tailing effects due to inset floodplains. We used a constant tracer input for the hyporheic zone because it took much longer to reach a steady state concentration.

2.2.2.7. In-Stream Structure Geometry

We based the geometry and spacing of in-stream structures on literature data, model grid constraints, and physical constraints. Spacing for in-stream structures typically varies from 10 m to 200 m and scales inversely with stream discharge [*Radspinner et al.*, 2010]. We calculated structure spacing for this study from cross vane spacing from two studies with similar drainage areas to Stroubles, scaled by discharge. The cross vane spacing was approximately 100 m [*Buchanan et al.*, 2012] and 150 m [*Crispell and Endreny*, 2009] for streams with baseflow discharge of 0.2 m^3/s (estimated from USGS gaging station near Bethel Grove, NY) and 0.05 m^3/s [*Crispell and Endreny*, 2009] respectively. For a summer baseflow of 0.025 m^3/s at Stroubles Creek this scaled to a spacing of approximately 15 m to ~~75~~ 75~~m,~~ m, with average of ~~45~~ 45~~m.~~ m. This translates to two in-stream structures over our 90 m reach where inset floodplain variation occurred. We used the 90 m reach instead of the full reach so solute retention could be directly compared between inset floodplains and in-stream structures.

The length of the in-stream structures (in the direction of channel flow) was 1 m due to the model grid resolution, and the width of the structure (perpendicular to channel flow) varied depending on how channel geometry intersected the square grid cells (2 m or 3 m). We set the height of the structure (0.3 m) using the methodology outlined by *Rosgen* [2001] that calculates the structure height based on the slope

of the cross vane arm from the bank to the channel. A vane slope of 4.5% (average of the 2% to 7% range specified by *Rosgen* [2001]) is used. The in-stream structures are located where inset floodplains are present to avoid additional negative impacts of construction activities [FISRWG, 1998], and because 4.5% slope from the pre-restoration bank to the channel would lead to unrealistic structure heights (i.e. >0.5 m) based on the geometry of Stroubles Creek [*Radspinner et al.*, 2010; *Wynn et al.*, 2010]. There is considerable variability in whether modeling studies do [*Endreny et al.*, 2011a; b] or do not [*Lautz and Siegel*, 2006; *Hester and Doyle*, 2008] extend the impervious part of the in-stream structure down into the sediment. For this study the structures extended 1 computational layer (~0.2 m) into the subsurface.

2.2.2.8. Sensitivity Analysis

We performed a total of 14 model runs to vary the hydraulic boundaries, hydraulic conductivity, inset floodplain length, and the presence of structures (Table 3). We also performed additional sensitivity analyses on n, ε_t, groundwater level (for summer baseflow stream stage), and the stream stage (for summer baseflow groundwater levels).

Table 3. Parameters varied for sensitivity analysis

Parameter	Description	Base Case	Minimum	Maximum	Presence of Structures
Surface and Groundwater Hydraulic Boundaries	1. Summer baseflow 2. Winter baseflow 3. Storm flow	Summer baseflow	NA	NA	Run both with and without
Sediment Hydraulic Conductivity (K)	Varied from that of a coarse sand to a silty-clay	1×10^{-6} m/s	1×10^{-8} m/s	1×10^{-4} m/s	Run with structures only
Inset Floodplain Length	Length of individual inset floodplain segment	20 m (F_b = 0.44)	0 m (F_b = 0.00)	90 m (F_b = 1.0)	Run with structures only[a]

[a]When varying the surface and groundwater hydraulic boundaries, the storm flow scenario was run with and without structures for the base case inset floodplain length (20 m). No effect was observed, so the analyses varying the floodplain length were only run with structures present.

2.2.3. Modeling Output

2.2.3.1. Flow and Storage

We separated the surface water domain into two distinct components (main channel and inset floodplain) and the groundwater into two components (hyporheic and non-hyporheic). The inset floodplains were delineated based on channel depth during storm flow (8.5 cm or less), with the exception of cells where the majority of the water flowing into a floodplain cell immediately flowed back into the

channel (i.e. 90% of the flow entering the inset floodplain immediately left again). With this delineation the flow into and out of the floodplains could be calculated using MIKE SHE flow output, and the volume could be calculated in the main channel and inset floodplain using the depth results. The solute mass stored in the inset floodplain and main channel were calculated similarly by multiplying the volume of water in each cell by its concentration of tracer.

Given the gaining nature of the reach, we considered all groundwater cells with greater than 10% concentration of conservative tracer to be potentially hyporheic [*Lautz and Siegel*, 2006], and double checked this delineation approach using particle tracking. Ten particles were added to any groundwater cell that was potentially hyporheic, and if any of those particles entered the channel downstream of the in-stream structure the cells were considered hyporheic and taken into account for volume and mass calculations. For the calculation of the mass of solute in groundwater cells, the porosity, cell volume, and concentration of solute tracer were taken into account. In-stream structure induced hyporheic flow was calculated by summing the flow for all hyporheic cells (as defined above) downstream of the in-stream structures (i.e. the upwelling portion of the hyporheic flow cell).

2.2.3.2. Residence Time

We output breakthrough curves from the model for solute moving in surface water (i.e. in the channel and inset floodplains) and in groundwater (upwelling portion of hyporheic flow cells). The time to 50%, 75%, and 99% of the steady state concentrations (i.e. t_{50}, t_{75}, and t_{99}) were calculated from the breakthrough curves, and were used to estimate residence times. We calculated t_{50}, t_{75}, and t_{99} in the main channel 2 m downstream of the downstream end of the full inset floodplain to approximate full reach residence times (Figure 1), and also at equal spaced intervals along the channel. The fractional increase in reach residence time due to the storage (RT_{FI}) was calculated by dividing the residence times for a given F_b by the residence time when $F_b = 0$.

We calculated residence times within individual inset floodplains and in-stream structure induced hyporheic flow cells using breakthrough curves at locations representing the center of solute mass flux exiting the storage zones and returning to the channel. The total mass flux leaving an inset floodplain was calculated by multiplying cell tracer concentrations by flow leaving each cell and summing. The same methods were used to calculate the mass flux in the hyporheic zone with the additional step of multiplying the result by the porosity. The methodology for selecting the specific cell that is the center of mass flux exiting the storage zones is given in the Results (Sections 2.3.1. and 2.3.3. for inset floodplains and hyporheic flow cells, respectively).

2.2.3.3. Fraction of Year that Storage Occurs

We estimated the portion of the year when in-stream structure induced hyporheic flow is expected at Stroubles Creek by performing a sensitivity analysis on the groundwater levels for summer baseflow scenarios. We performed the sensitivity analysis on the groundwater because it is the strongest controlling variable of whether hyporheic flow will occur [*Cardenas and Wilson*, 2006; *Lautz and Siegel*, 2006; *Hester and Doyle*, 2008; *Sawyer and Cardenas*, 2012]. We then calculated what percent of the year the groundwater levels were within the levels where hyporheic flow was expected. An additional sensitivity analysis was performed on the baseflow stream stage to estimate for what stream stages surface storage due to in-stream structures is expected. We estimated the portion of the year where inset floodplains were active by calculating the total time that the stream stage measured at the stream gage exceeded the inset floodplain elevation (0.5 m).

2.3. Results

2.3.1. Exchange Flows with Storage Zones

For storm flow scenarios, water primarily flowed from the main channel into the inset floodplains over the upstream half of their shared boundary, and from the floodplain back into the channel over the downstream half (Figure 4). The fraction of channel flow that entered the inset floodplain ($Q_{F\text{-}FP}$) across the entire reach increased non-linearly with fraction of bank with inset floodplain (F_b, Figure 5). $Q_{F\text{-}FP}$ plateaued when F_b was 0.67 (inset length of 30 m) with approximately 56% of the channel flow spending some time in the floodplains. During summer and winter baseflow scenarios there was no surface water flow into or out of the inset floodplains.

Stroubles Creek was gaining during baseflow scenarios in both the summer (Figure 6a) and winter (Figure 6b), but was more gaining in the winter due to higher groundwater levels. In-stream structure induced hyporheic flow (flow entering groundwater upstream of structures and re-entering stream downstream of structures) was higher in summer than in winter due to these differences in background groundwater levels. In fact, there was no structure induced hyporheic flow in winter, although the magnitude of upwelling directly upstream of the structures decreased and the magnitude of upwelling directly downstream of the structures increased relative to when no structures were present. During storm flow the stream was generally losing, and the water depths in the channel upstream and downstream of in-stream structures were the same such that in-stream structure induced hyporheic retention did not occur. There was a linear increase in the fraction of channel flow that entered the in-stream structure induced hyporheic zone ($Q_{F\text{-}HZ}$) with hydraulic conductivity (K) for the summer baseflow scenarios (Figure 7).

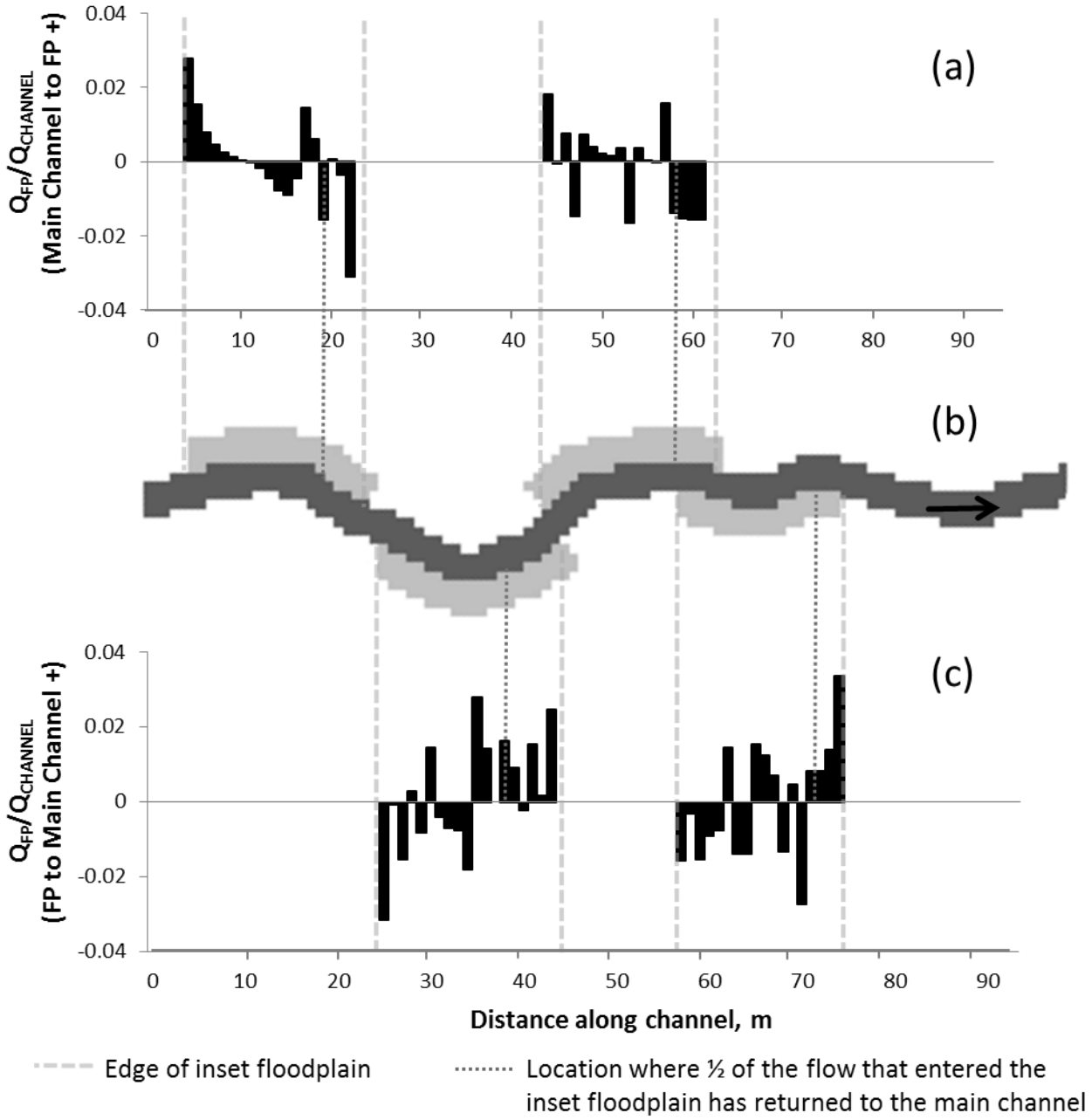

Figure 4. Exchange flow between main channel and inset floodplains (Q_{FP}) normalized by the channel flow at the upstream boundary ($Q_{CHANNEL}$) versus distance along stream for the east bank (a) and west bank (c) for storm flow scenario. The digitized main channel of Stroubles (dark gray) and inset floodplains (light gray) are also displayed with arrow displaying channel flow direction (b). To make the direction of flow more visually intuitive, y-axes of plots in panels a and c are reversed such that flow out of the channel into the floodplain is positive in panel a and negative in panel c. This causes all flow moving east across the main channel-inset floodplain boundary to be displayed as positive, and all flow moving west to be displayed as negative.

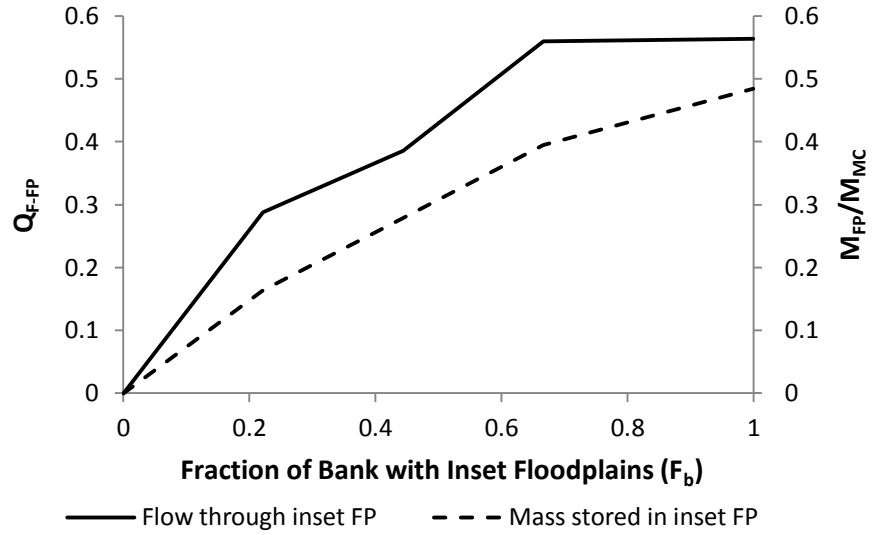

Figure 5. Fraction of surface water flow that ~~enters~~ entered inset floodplains (Q_{F-FP}) and total mass stored in inset floodplains (M_{FP}) normalized by the mass stored in the main channel (M_{MC}) versus fraction of bank with inset floodplain (F_b). Both Q_{F-FP} and M_{FP}/M_{MC} are for storm flow scenarios.

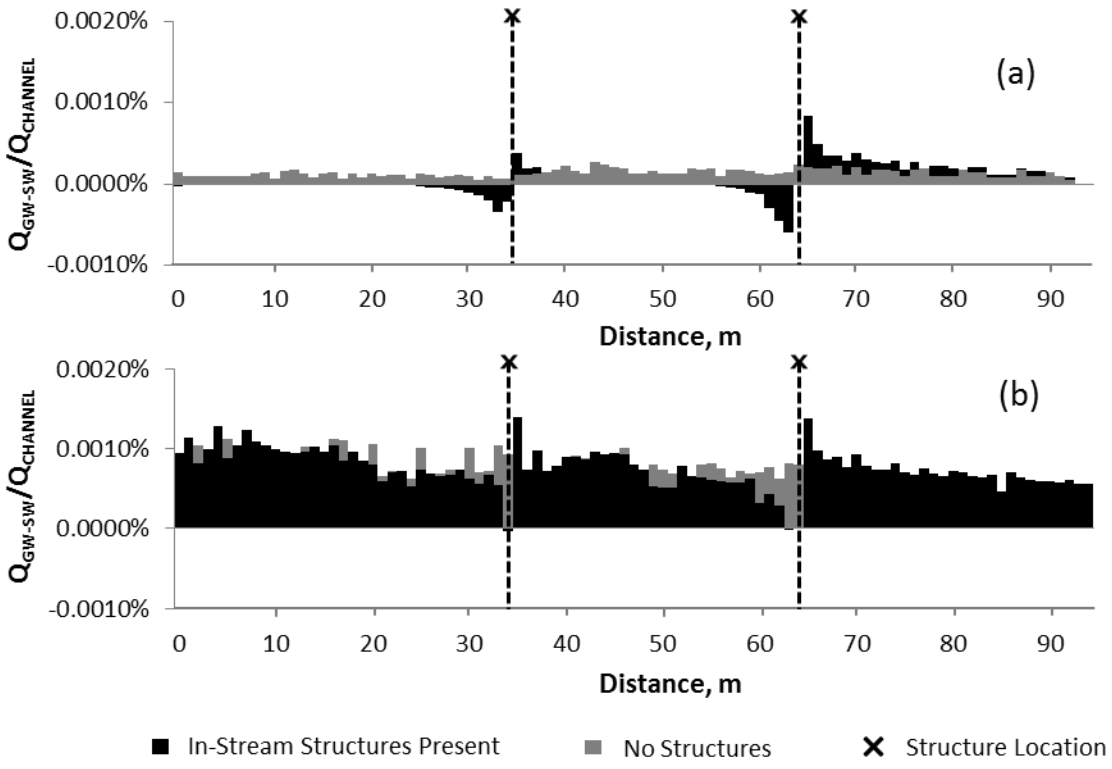

Figure 6. Flow from groundwater to stream (Q_{GW-SW}) normalized by the channel flow at the upstream boundary ($Q_{CHANNEL}$) versus distance along channel for summer baseflow (a) and in winter baseflow (b) scenarios.

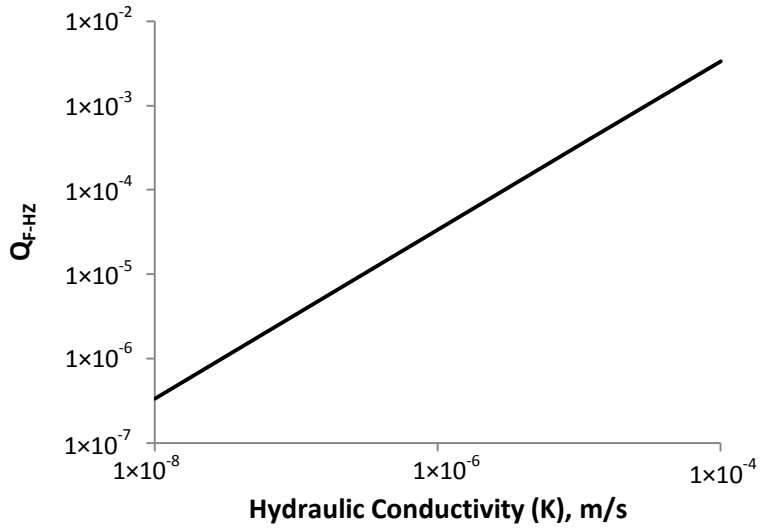

Figure 7. Fraction of total flow in the channel that ~~enters~~ entered in-stream structure induced hyporheic zone ($Q_{F\text{-}HZ}$) versus hydraulic conductivity (K) for summer baseflow scenarios.

2.3.2. Mass Storage

Mass storage in inset floodplains increased with F_b, with a slight decrease in slope as F_b approached 1.0 (Figure 5). A ratio of the mass stored in the main channel to the mass in the inset floodplain is used to illustrate how the ~~magnitude of storage~~ floodplain storage ~~compared~~ compares to ~~the~~ storage in the channel. Less mass was stored in the floodplains than was stored in the channel for all F_b, with the mass in the floodplains for F_b = 1.0 (full inset floodplain) approaching 50%. For the storm flow scenario the solute concentration throughout the floodplains is the same as the upstream boundary condition (1 g/m^3). As a result the solute mass stored in the inset floodplains (normalized for main channel mass storage) is nearly identical to the floodplain water volume storage (normalized for main channel volume).

For summer baseflow scenarios, the steady state volume of the in-stream structure induced hyporheic zone (within the hyporheic flow cells induced by the two structures) and mass of solute stored in the hyporheic zone were identical for all K. Under such steady state conditions there was 3.9 times more water (by volume) and 2.8 times more mass of solute stored in the hyporheic zone than in the channel. However, due to high residence times, and the fact that hyporheic flow does not exist at certain times of year (e.g., winter), actual storage in the hyporheic zone is generally expected to be less than this theoretical steady-state summer maximum. Such residence time-limited partial hyporheic storage increased with the duration that summer baseflow hydraulic conditions persisted at approximately steady state and also with K (Figure 8). For 10 to 60 days of summer baseflow hydraulic conditions, storage for the lowest K (1×10^{-6} m/s or less) was below 15% of the mass stored in the channel, and the greatest storage consistently occurred for the highest K (1×10^{-4} m/s).

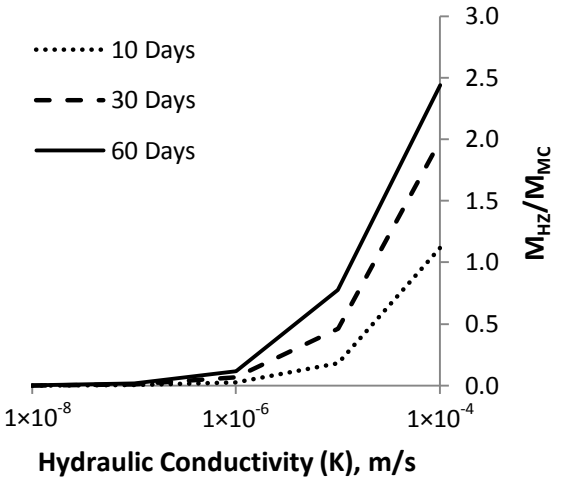

Figure 8. Mass stored in the hyporheic zone (M_{HZ}) normalized by mass stored in the main channel of the stream (M_{MC}) for varying hydraulic conductivities (K) and different durations of steady state summer baseflow conditions.

2.3.3. Residence Times

Channel residence times in the modeled reach were longest for summer baseflow scenarios and shortest for storm flow scenarios (Figure 9). Residence times increased in the presence of structures during summer and winter baseflow scenarios, but did not for the storm flow scenario. The largest change in median residence time due to adding structures occurred for summer baseflow (factor of 3), followed by winter baseflow (factor of 2). While the breakthrough tracer curves did not change for the storm flow scenario when structures were added, the time to reach a steady state concentration at the downstream location (and return to baseline) increased as F_b increased (Figure 10).

F_b significantly affected reach residence times during storm flow scenarios, particularly the upper end of the residence time distribution. The fractional increase in reach residence time (RT_{FI}) for the time to 50%, 75%, and 99% of the steady state concentrations (i.e. t_{50}, t_{75}, and t_{99}) increased relative when no floodplains were present (Figure 11). t_{99} linearly increased with F_b, while both the t_{50} and t_{75} leveled off at $F_b = 0.67$ and $F_b = 0.44$, respectively.

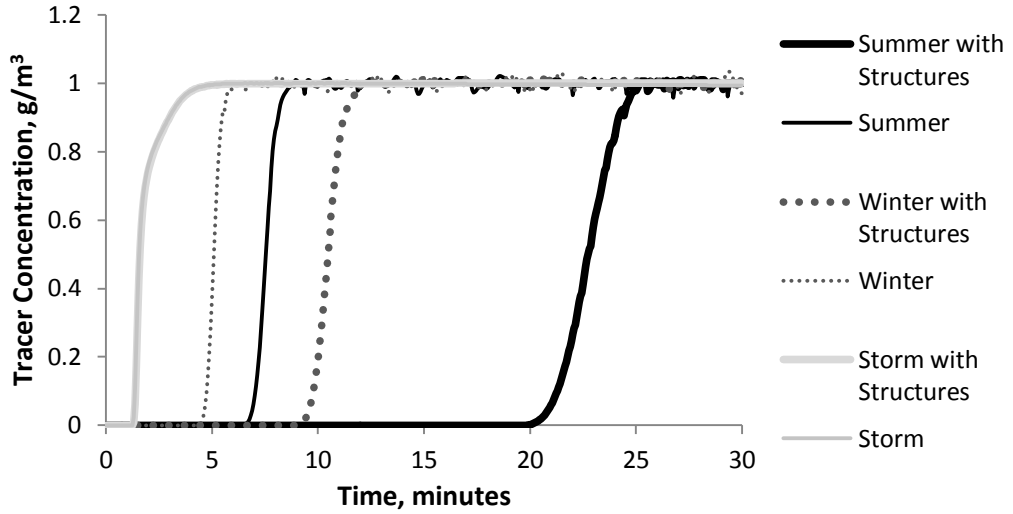

Figure 9. Breakthrough tracer curves in the thalweg at the downstream model boundary for summer baseflow, winter baseflow, and storm flow scenarios with and without structures. For all scenarios displayed the fraction of bank with inset floodplains is 0.44.

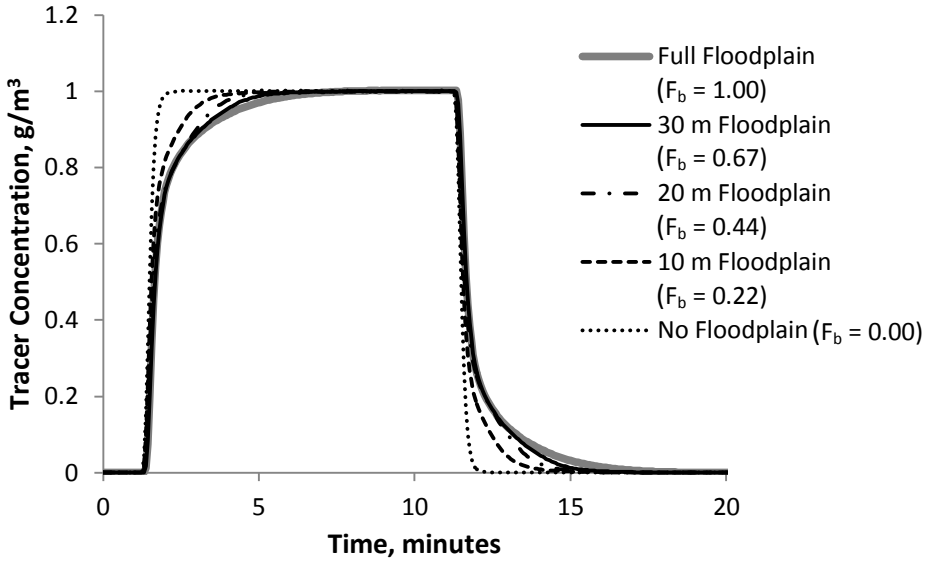

Figure 10. Breakthrough tracer curves for storm flow scenarios in the thalweg of the stream at the downstream boundary for varying fraction of bank with inset floodplain (F_b).

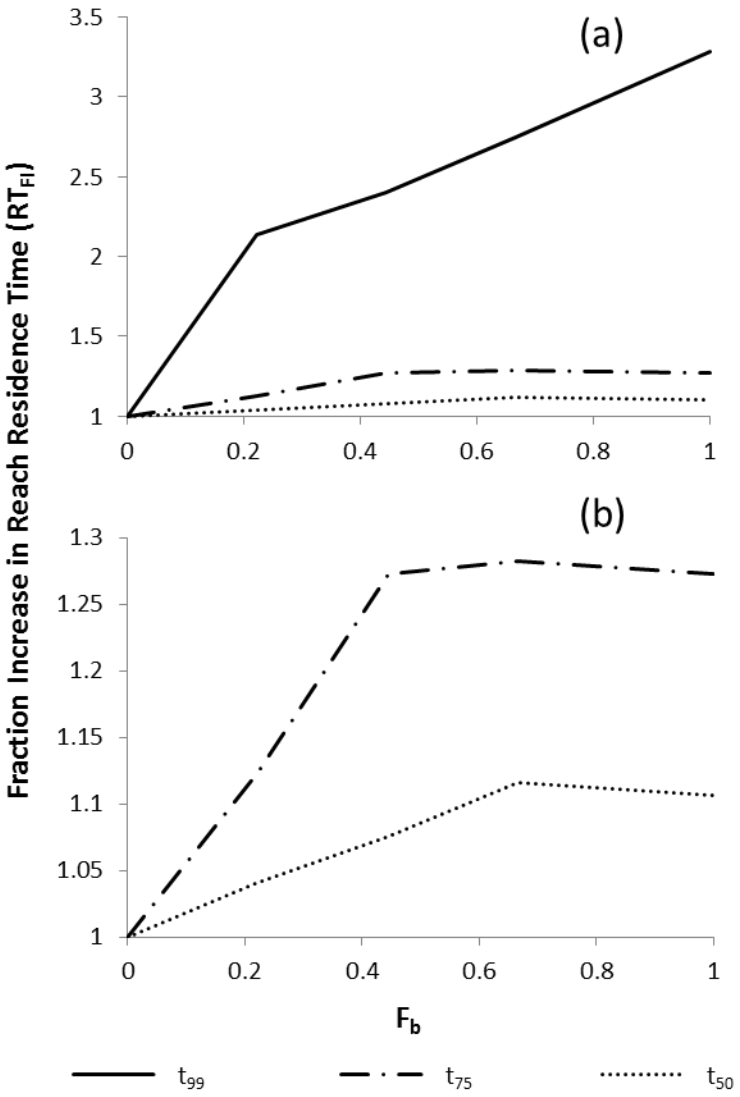

Figure 11. Fractional increase in the reach residence time (RT_{FI}) versus fraction of bank with inset floodplain (F_b) for storm flow scenarios. The RT_{FI} is displayed for time to 99%, 75%, and 50% of steady state concentration (t_{99}, t_{75}, and t_{50}) at downstream boundary of reach (a), and zoom in of t_{75}, and t_{50} (b). The residence times are normalized relative to the condition without inset floodplains.

The t_{50} RT_{FI} from adding inset floodplains increased with distance along the channel (Figure 12). This increase was generally linear ($0.94 < R^2 < 0.97$) with slight undulations associated with the complex flow behavior of the floodplains as well as their locations along the stream. The RT_{FI} also increased with F_b for values of F_b from 0.00 to 0.67. The RT_{FI} is then similar for $F_b = 0.67$ and $F_b = 1.0$, with variation in which is greatest depending on the location along the channel.

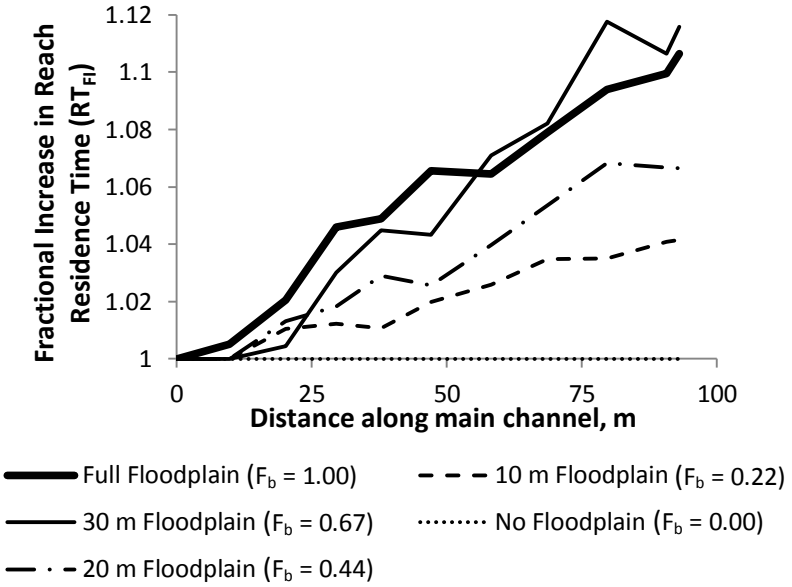

Figure 12. Fractional increase in reach residence time (RT_{FI}) for the time to 50% concentration (t_{50}) due to adding inset floodplains versus distance along main channel. Different lines indicate different floodplain lengths and fraction of bank with inset floodplain (F_b) values. The distance along the main channel begins 1 m upstream of the start of the full floodplain, and ends 2 m downstream of the end of the full floodplain.

We also evaluated residence times within individual inset floodplains. We calculated the center of mass flux exiting the floodplain by locating where half of the total mass flux that entered an inset floodplain segment had exited the inset floodplain and re-entered the channel (Figure 4). For an inset floodplain length of 20 m (F_b = 0.44) the center of mass flux exiting each individual inset floodplain was located between 70% and 90% of the floodplain length downstream from the upstream end of the floodplain (Figure 4). This percentage varied for other inset floodplain lengths, but was always between 60% and 90%. As the inset floodplain length (and consequently F_b) increased, it took longer for steady state solute concentrations to be reached at the center of mass flux exiting the floodplain (Figure 13). Compared to the location of the center of mass flux leaving the floodplain, breakthrough tracer curves toward the start of the floodplains were steeper and reached steady state faster (not shown), while those toward the end were less steep and reached steady state slower (also not shown). Breakthrough tracer curves shown in Figure 13 are for the northernmost inset floodplain segment so the effect of travel time in the channel is minimized. Nevertheless, to more accurately estimate inset floodplain residence times we corrected the inset floodplain t_{50} by subtracting the channel t_{50} for the adjacent channel for all inset floodplain segments. The average residence times within individual inset floodplains increased with the floodplain length (Figure 14), with a range in t_{50} of approximately 0.8 minutes to 1.4 minutes.

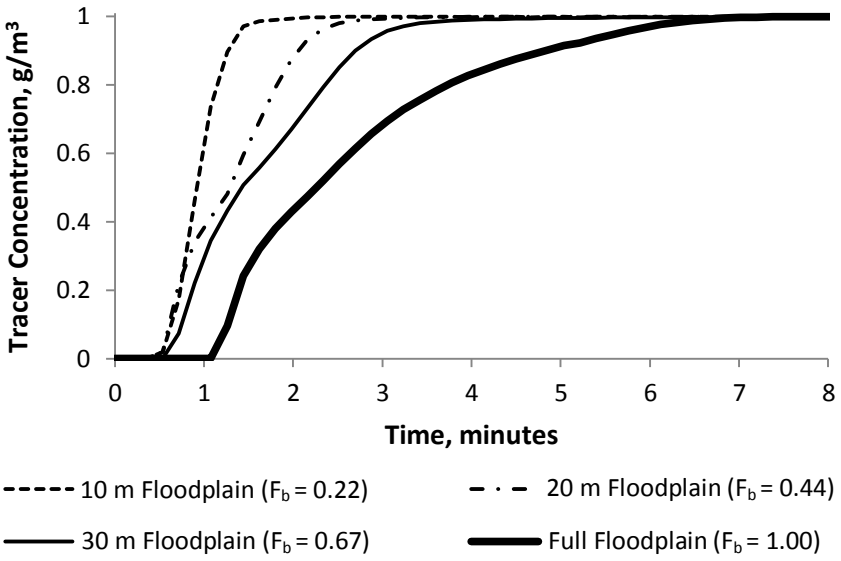

Figure 13. Breakthrough curves for storm flow scenarios at the center of mass flux exiting the most upstream inset floodplain for a range of fraction of bank with inset floodplains (F_b). To give a better estimate of the residence time within the inset floodplain the breakthrough tracer curves were taken one cell away from the interface between the main channel and inset floodplain.

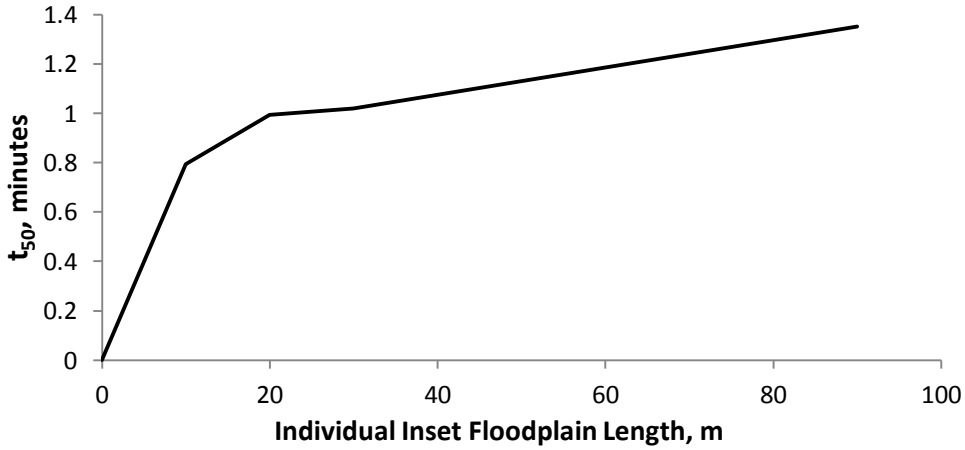

Figure 14. Time to 50% steady state concentration (t_{50}) within a single inset floodplain versus inset floodplain length. The t_{50} for each of the four inset segments was calculated and the average value is given for each floodplain scenario.

Structure-induced hyporheic flow cells have a wide range of residence times [*Menichino and Hester*, 2013]. The majority (60%) of the mass flux reentering the channel from the structure-induced hyporheic flow cells did so within 1 m downstream of the in-stream structures for steady state solute concentrations (Figure 15). Prior to steady state, this proportion is even higher. We therefore estimated the t_{50} in the hyporheic zone as the flux-weighted average t_{50} from the breakthrough tracer curves for cells upwelling into the stream within 1 m of the in-stream structures (3 cells at the upstream structure and 2

cells at the downstream structure). The breakthrough tracer curves with a t_{50} closest to the flux-weighted average t_{50} of these 5 hyporheic cells (i.e. the model cells just downstream of each structure, Figure 15) are plotted for visualization (Figure 16). It took longer to reach the steady state solute concentration for low K, with steady state reached at 40 days for K = 1×10^{-4} m/s, and an increase in concentration of less than 1% over 90 days for K = 1×10^{-7} m/s. The t_{50} increased from approximately 6 to 300 days as K increased from 1×10^{-4} m/s to 1×10^{-6} m/s (Figure 17).

2.3.4. Fraction of Year that Storage Occurs

For summer baseflow scenarios, in-stream structure induced hyporheic flow was not expected when the depth of the water table below ground surface decreased by more than 50% of the current summer groundwater conditions (e.g., if the phreatic surface was altered from 1 m below the ground surface to 0.5 m below the ground surface). For the most recent full year of groundwater data available (December 2009 to December 2010), the in-stream structures ~~we~~ modeled would induce hyporheic exchange for approximately 20% of the year (during dry periods in the summer and early fall). By comparison, the inset floodplains were only active when the stream stage was higher than the inset floodplain elevation (0.5 m), or approximately 1% of the year for the most recent full year of stream stage data (May 2011 to May 2012). The surface storage due to in-stream structures increased the channel median residence time by at least 10% for flow depths up to 0.35 m (all below the stage required to inundate inset floodplains, 0.5 m). Surface retention due to in-stream structures was expected for 90% of the year, also based on data from May 2011 to May 2012. Surface retention due to in-stream structures was not expected during storm events, but periods where flow was high enough to prevent surface retention generally occurred for less than 24 consecutive hours.

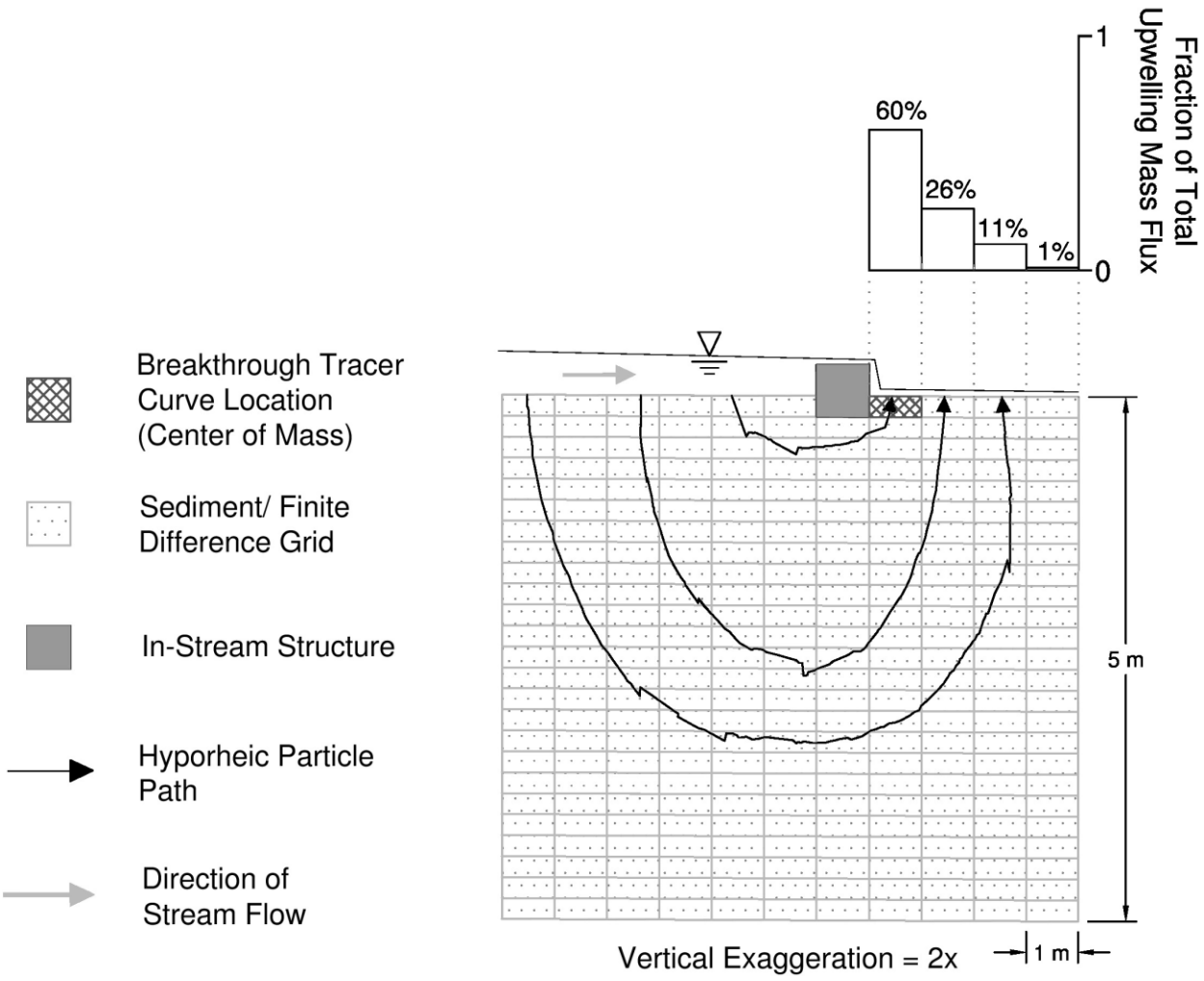

Figure 15. Location where breakthrough curves and residence times in the in-stream structure induced hyporheic zone are output from the model. The fraction of total mass flux exiting the hyporheic zone is shown for cells 1, 2, 3 and 4 meters from center of the in-stream structure at steady state for summer baseflow scenarios. Hyporheic flow paths are from particle tracking.

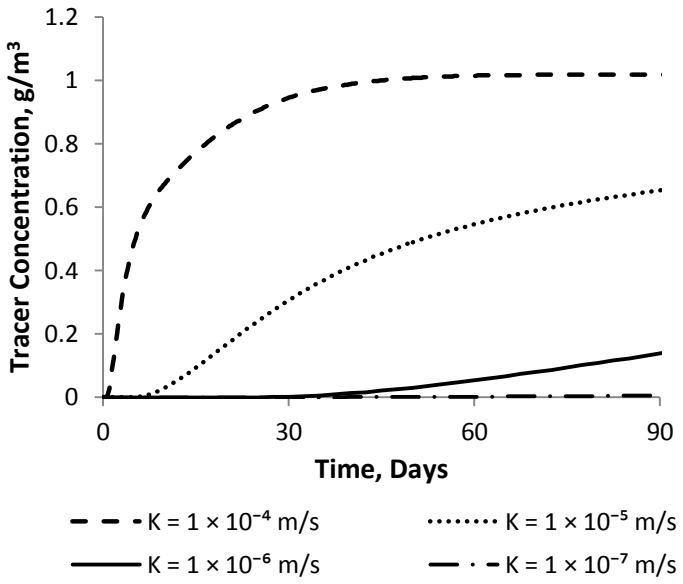

Figure 16. Breakthrough curves at upwelling cell 1 m downstream of in-stream structure for summer baseflow scenario with varying hydraulic conductivities (K). See Figure 15 for why this particular model cell was chosen. K = 1×10^{-8} m/s is omitted because there is no measurable change in concentration over 90 days.

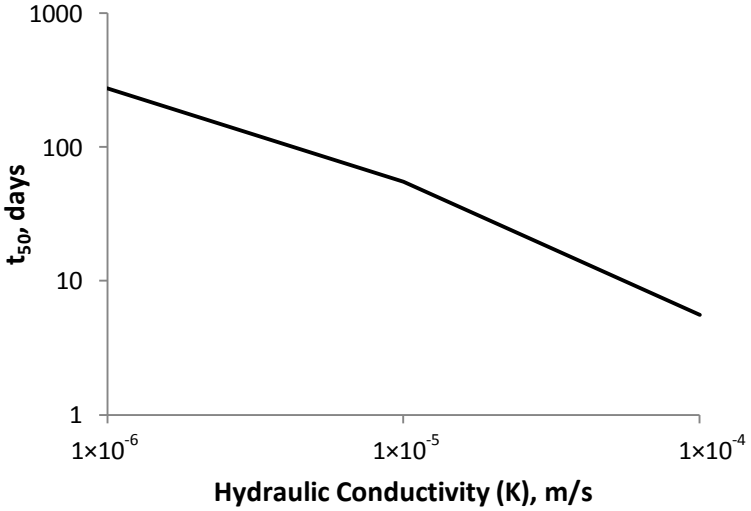

Figure 17. Median residence time (t_{50}) in the in-stream structure induced hyporheic zone for summer baseflow scenarios versus hydraulic conductivity (K). The lowest K (i.e. 1×10^{-7} m/s and 1×10^{-8} m/s) are omitted because t_{50} was unrealistically high (over a year).

2.4. Discussion

2.4.1. Natural Controls on Hydraulics and Solute Retention

In-stream structure induced hyporheic flow occurred for summer but not winter baseflow scenarios (Figure 6). Such seasonal variation is consistent with previous studies [*Wondzell and Swanson*, 1996]. This is due more to variation in groundwater levels than variation in surface water levels, as

hyporheic flow generally only occurs under neutral to moderately gaining groundwater conditions, because highly gaining or losing streams inhibit hyporheic exchange [*Cardenas and Wilson*, 2006; *Lautz and Siegel*, 2006; *Hester and Doyle*, 2008; *Sawyer and Cardenas*, 2012]. Regardless of groundwater levels, in-stream structure induced hyporheic flow was eliminated during storm flow scenarios when the stream stage was more than twice the height of the in-stream structure (Figure 9). This caused the head drop across the in-stream structure to approach the stream slope eliminating the hydraulic gradient that drives hyporheic flow, consistent with *Crispell and Endreny* [2009] and *Hester and Doyle* [2008].

Flow and residence times in the in-stream structure induced hyporheic zone during summer baseflow scenarios were highly dependent on the hydraulic conductivity (K) of the stream sediment (Figure 7 and 17), consistent with prior work [*Boulton et al.*, 1998; *Hester and Doyle*, 2008; *Sawyer et al.*, 2011; *Menichino and Hester*, 2013]. For the range of stream sediment K used in this study, the hyporheic zone did not have a significant effect on overall stream reach residence times because the proportion of surface flow that cycled through the hyporheic zone was so small (Figure 7). The dominant influence of surface storage on reach retention or transient storage is consistent with field studies [*Ensign and Doyle*, 2005; *Jin and Ward*, 2005; *Stofleth et al.*, 2008]. Although not the focus of this study, surface storage also occurred behind in-stream structures during baseflow due to a decrease in channel flow velocity in the backwater areas upstream of structures, consistent with *Ensign and Doyle* [2005]. The primary control on surface storage upstream of in-stream structures (during summer baseflow) and in inset floodplains (during storm flow) is stream stage (Figure 9). Streams with flashy hydrographs (e.g., those effected by agriculture or urbanization) are the best candidates for inset floodplain restoration since the floodplains will be active more often [*Royall et al.*, 2010].

2.4.2. Stream Restoration Design Controls on Solute Retention

2.4.2.1. In-Stream Structures

In-stream structures are useful for inducing hyporheic flow only where certain conditions are met for a reasonable amount of the year. These conditions include near-neutral groundwater environments, baseflow stream level, and K sufficiently large for significant proportion of the stream flow to enter the hyporheic zone. These groundwater and K requirements for hyporheic retention are consistent with other hyporheic studies in streams and rivers [*Lautz and Siegel*, 2006; *Hester and Doyle*, 2008; *Wondzell*, 2011; *Sawyer and Cardenas*, 2012]. Such conditions are necessary but not sufficient to insure water quality effects, as all reactant must also be present [*Schnoor*, 1996] and there must be sufficient residence time in the storage zones [*Zarnetske et al.*, 2011; *Zarnetske et al.*, 2012].

A maximum of only 0.3% of surface stream flow traveled through the in-stream structure induced hyporheic zone for a 90 m reach and our maximum K of 1×10^{-4} m/s (Figure 7), but the hydrologic effects

of in-stream structure induced hyporheic flow are additive. Therefore, restoring a longer reach with the same structure spacing along the channel (i.e. structure density) can lead to a proportionally greater fraction of flow entering the hyporheic zone. We derived a simple empirical equation to estimate this scaling effect by using the relationship shown graphically in Figure 7:

$$Q_{F-HZ} = \frac{(9.2\times10^{-3})KL_R}{Q_{CHANNEL}} \quad (5)$$

where $Q_{F\text{-}HZ}$ is the fraction of stream flow that enters the in-stream structure induced hyporheic zone (dimensionless), $Q_{CHANNEL}$ is surface water flow in the channel (m^3/s), K is the hydraulic conductivity (m/s), and L_R is the length of restored reach (m) with two 0.3 m in-stream structures every 90 ~~m,~~ m, all for summer baseflow conditions at Stroubles Creek. As expected, $Q_{F\text{-}HZ}$ increases proportionally with both K and L_R. Equation (5) can be written more generally as:

$$Q_{F-HZ} = \frac{(\propto K)D_s L_R}{Q_{CHANNEL}} \quad (6)$$

where α is a hyporheic hydraulic coefficient (m^2), D_s is the structure density (#/m), and L_R is the length of restored reach with in-stream structure density D_s (m). For this study α is 4.6×10^{-3} m (from linear regression), D_s is 2/90 m^{-1}, L_R is 90 ~~m,~~ m, and $Q_{CHANNEL}$ is 0.025 m^3/s. This can be used to estimate the length of channel with structures necessary to cycle a given proportion of stream water through the hyporheic zone. For example, cycling all stream water through the in-stream structure induced hyporheic zone once ($Q_{F\text{-}HZ}$ = 1) at Stroubles Creek would require approximately 3,000 km of restored channel (for K = 1×10^{-6} m/s). Halving the structure density or doubling the channel flow rate would then double the required restoration length. These lengths of channel seem long and prohibitive from the perspective of the current stream restoration paradigm where small reaches are restoration at scattered locations throughout a given watershed. However, if natural riparian areas are restored, natural tree recruitment processes would create structures in larger numbers over larger areas whose effect might approach the levels discussed here. Required length of stream would also be substantially less in regions with higher K. Further, since in-stream structure induced hyporheic flow is superimposed upon naturally occurring hyporheic flow, a larger fraction of stream flow is expected to spend time in the hyporheic zone than estimated here.

From Darcy's Law we expect that α in Equation (6) depends linearly on the hydraulic gradient across the in-stream structures and the surface area of upwelling groundwater. The structure height is the primary control on the hydraulic gradient for neutral groundwater conditions. However, if the stream is highly gaining or losing the hydraulic gradient from the groundwater to the stream is larger than that

induced by the in-stream structure. This effectively makes the hydraulic gradient across the in-stream structure (and therefore α) zero, in agreement with [*Hester and Doyle*, 2008]. Due to the relatively narrow range of groundwater levels (e.g., relatively neutral conditions) where in-stream structures are expected to induce hyporheic flow and spatial variability in K, scaling must be done carefully. Changes in the groundwater levels or K alter $Q_{F\text{-}HZ}$, so extrapolating Equation (6) beyond where both parameters are known is not advised. The effects of bed heterogeneity and anisotropic conditions lead to additional variability [*Salehin et al.*, 2004; *Sawyer and Cardenas*, 2009]. In-stream structures also induced surface water storage by decreasing the stream velocity for a variety of flows, with the amount of storage decreasing as the stage increased (Figure 9). This retention should also scale with length of restored reach, but it was not our focus here since the water does not leave the main channel.

2.4.2.2. Inset Floodplains

Inset floodplain length and therefore fraction of bank with floodplains (F_b) are key parameters controlling solute retention. As these parameters increased, the fraction of stream flow that entered inset floodplains ($Q_{F\text{-}FP}$), the fractional increase in overall reach residence times (RT_{FI}), the mass stored in inset floodplains, and the residence time within individual inset floodplain segments all increased (Figures 5, 11, and 14). However, all of these trends were nonlinear, and leveled off to varying degrees as floodplain length or F_b increased. For example, $Q_{F\text{-}FP}$ and RT_{FI} (for t_{50} and t_{75}) level off at F_b less than 1.0 (Figure 5 and 11). This was due to the relationship between momentum and topographic controls on flow into inset floodplains. Channel flow generally has greater momentum (depth and velocity) at the outside of meander bends [*Leopold and Wolman*, 1960], resulting in flow for the full floodplain (F_b = 1.0) to be driven into the floodplains primarily at the upstream end of meanders with this flow reentering the channel ~~and~~ at the downstream end [*Naish and Sellin*, 1996]. The smaller inset floodplain segments (F_b < 1) added topographic controls to this phenomenon, as flow could only enter the inset floodplains where they exist and was forced to reenter the channel where they ended. This topographic control is what caused the Q_F and RT_{FI} to increase from F_b = 0.00 to F_b = 0.67. For F_b = 0.67 the flow is not limited by the topographic controls, resulting in similar $Q_{F\text{-}FP}$ and RT_{FI} to F_b = 1.0.

The nonlinearities in these trends have economic implications for stream restoration. Installing inset floodplains on a 90 m reach with a F_b of either 0.67 or 1.0 yielded identical $Q_{F\text{-}FP}$ of 56%, as well as similar increases in the t_{50} and t_{75}. Therefore, assuming floodplain restoration cost scales with length of bank restored, a longer stream reach could be restored with F_b = 0.67 than could be with F_b = 1.0 for the same price. In other words, inset floodplains installed along a longer reach with F_b = 0.67 would lead to a higher RT_{FI} for the t_{50} and the t_{75} than a full inset floodplain (F_b = 1.0) along a shorter reach. This recommendation contradicts recent guidance for restoration practitioners that predicts water quality

improvements based on the length or restored reach, not giving credit for strategic gaps [*Schueler and Stack*, 2012]. There is also a trend in recent stream restoration projects to install floodplains with $F_b = 1.0$ [*Kaushal et al.*, 2008; *Roley et al.*, 2012b; *Roley et al.*, 2012a].

We found that the RT_{FI} for the t_{50} caused by adding inset floodplains increased with length of the overall restored reach (Figure 12). This increase was linear with an R^2 value of 0.94 or greater for all F_b. We used this result to derive a simple empirical scaling equation:

$$RT_{FI} = 1 + L_R\beta \tag{7}$$

$$\beta = \begin{cases} 0.0018(F_b) & \text{if } F_b \leq 0.67 \\ (0.0018)(0.67) - 0.0002(F_b - 0.67) & \text{if } F_b > 0.67 \end{cases} \tag{8}$$

where RT_{FI} is the fractional increase in the reach residence time due to inset floodplain installation (dimensionless), L_R is the length of reach where restoration takes place (m), β is the inset floodplain-main channel exchange coefficient (m^{-1}) defined by Equation (8), and F_b is the fraction of bank with inset floodplains. This can be used to estimate the length of channel with inset floodplains required to increase the overall stream residence time by a certain amount during storm flow. For example, for $F_b = 0.67$ it would require approximately 200 m of restored channel at Stroubles Creek to increase the overall reach residence time by 20% ($RT_{FI} = 1.2$). Because this type of calculation involves extrapolation beyond our modeled reach, it should be viewed as an estimate, but it is a useful heuristic to understand inset floodplain restoration effects on stream residence times.

We found that the slope of RT_{FI} versus reach length increased with F_b from $F_b = 0.00$ to $F_b = 0.67$ and then almost levels off between $F_b = 0.67$ and $F_b = 1.0$ (Figure 12). We used the β term in Equations (7) and (8) to account for this non-linear increase in slope with F_b. This nonlinearity (leveling off) was due to the relationship between the momentum of channel water and topographic controls discussed previously in this section. We anticipate variation in β from one stream to another based on channel geometry.

2.4.3. Complementary Nature of Inset Floodplains and In-Stream Structures

One of the key findings of this study is that inset floodplains and in-stream structures retained solutes in dramatically different and highly complementary ways as quantified by the various storage metrics (Table 4). For example, while inset floodplains retained solutes for storm flow scenarios, in-stream structures retained solutes for summer baseflow scenarios. Due to these hydraulic differences, retention in the hyporheic zone occurred for a larger portion of the year than retention in floodplains. On the other hand, floodplains induced higher exchange flows during storm flow scenarios than structure

induced hyporheic flow during baseflow scenarios. At least 10 km of stream with two structures every 90 m would be needed to cycle the same amount of water through the hyporheic zone as is cycled in the inset floodplains of our 90 m model reach (depending on K and F_b).

Table 4. Comparison of retention induced by in-stream structures and inset floodplains [a]

	Structure-Induced Hyporheic Zone	Inset Floodplain
Time when dominant retention element	Baseflow	Storm Flow
Approximate % of year when engaged	**20%**	1%
Fraction of flow that enters storage zone (Q_F)	0.00002 – 0.002	**0.3 – 0.6**
Steady State Storage (M/M_{MC})	**2.8**	0.2 – 0.5
Median residence time in storage zone (t_{50})	**6 – 300 days**	0.8 to 1.4 minutes
Fractional increase in reach residence time (RT_{FI})	1.0	**1.1 – 3.3**

[a]Bold text indicates the restoration practice that leads to more retention for each metric.

The mass stored in the in-stream structure induced hyporheic zone at steady state solute concentrations was up to an order of magnitude larger than that stored in inset floodplains at steady state. Nevertheless, mass storage in the hyporheic zone can be either greater or less than in inset floodplains depending on season and K because steady state is reached within minutes for inset floodplains (Figure 10) but takes days to months in the hyporheic zone (Figure 16). Residence times in the hyporheic zone were several orders of magnitude larger than those in the inset floodplains (consistent with *Helton et al.* [2012]) and are therefore expected to lead to more complete reactions in many cases. Lastly, the ~~RT_{FI}~~ reach residence times increased due to storage in inset floodplains, but due to low $Q_{F\text{-}HZ}$ the ~~RT_{FI}~~ reach residence time did not change as a result of in-stream structure induced hyporheic storage (i.e. $RT_{FI} = 0$).

While in-stream structured induced hyporheic zones and inset floodplain storage areas were complementary (Table 4), neither storage zone is expected to have sufficient residence times and sufficient percent of flow *simultaneously*. This may limit the effect of these stream restoration practices on water quality. For example, the fraction of stream flow that ~~enters~~ entered the hyporheic zone for the 90 m reach modeled in this study (Figure 7) is too low to have a significant impact on surface water quality. Yet the residence times (Figure 14) are likely long enough for reactions of pollutants (e.g., excess nitrate) to occur in the induced hyporheic zones [*Zarnetske et al.*, 2011; *Zarnetske et al.*, 2012]. In contrast, inset floodplains retain a significant percent of the stream flow (Figure 5). Yet the average

residence times in the inset floodplains are on the order of minutes (Figure 14), and are generally too low to expect full reactions of pollutants to occur [*Zarnetske et al.*, 2011; *Zarnetske et al.*, 2012]. Nevertheless, higher sediment K and restoring a longer reach can increase the flow into the hyporheic zone. Similarly, there are slow moving areas of water at the fringe of the inset floodplains that have larger residence times than the average, and planting thick vegetation could further increase residence times. Opportunities for reactions that affect surface water therefore likely occur only in specific locations and at specific times during the year. These locations and times have been referred to as hotspots and hot moments [*McClain et al.*, 2003].

Surface storage due to inset floodplains occurred for only ~1% of the year in this study (Table 4), leaving seemingly little chance for a water quality effect. Yet even this level of engagement is substantially more than bankfull floodplains that are typically inundated once every 1 to 2 years [*Soar and Thorne*, 2011]. Furthermore, during storm flow events far more than 1% of annual stream flow (e.g., ~36% during the 10 days with the greatest flow [*USGS*, 2013]) and between 40% and 90% of annual pollutant loading occurs [*Owens et al.*, 1991; *Pionke et al.*, 1999; *Royer et al.*, 2006], making inset floodplains potentially more important than inundation frequencies suggest. Several studies suggest that restoration efforts should focus on retention during these high pollutant loading yet low probability events [*Bayley*, 1991; *Hein et al.*, 2003; *Rohde et al.*, 2006]. This is due in part to additional benefits of floodplains for improving water quality including buffering of contaminated groundwater and surface runoff [*Haycock and Burt*, 1993], and an increase in soil mineralization rates in floodplain sediments [*Noe et al.*, 2013].

By contrast, in-stream structure induced hyporheic retention occurred for approximately 20% of the year at Stroubles Creek (summer baseflow) while surface storage behind structures reduced overall reach velocities for over 90% of the year. Depending on the groundwater conditions for a given stream, these percentages could vary considerably. Several studies have suggested that the hyporheic zone can be used for water quality mitigation [*Hester and Gooseff*, 2010; *Daniluk et al.*, 2012]. From this study we hypothesize that in-stream structure induced hyporheic flow may augment naturally occurring hyporheic flow [*Nagaoka and Ohgaki*, 1990; *Storey et al.*, 2003; *Boano et al.*, 2006] leading to a small improvement in water quality over a relatively large portion of the year. In other words, restoration induced hyporheic flow is probably best able to address low levels of contaminants that linger after other approaches (e.g., stormwater detention, and wastewater treatment plants) have already removed the great majority. Even in such low-level situations, relatively high K and relatively long distances of restored stream are probably necessary for a measureable effect on water quality. Future studies will need to better quantify what K and length of restored stream are necessary, and these would be expected to vary among different contaminants and biogeochemical conditions.

2.4.4. Evaluation of Key Parameters Estimated in the Field

We performed a sensitivity analysis to estimate the impact of the selection of the Manning's roughness coefficient (n) and the transverse mixing coefficient for surface water (ε_t) used for this study. We varied n for the main channel and inset floodplain across a reasonable range of values (0.025 to 0.05 for the main channel and 0.05 to 0.1 for the inset floodplain) [*McCuen*, 2005]. Storm flow models were run with all combinations of the minimum, maximum, and base n for the main channel and inset floodplain. The maximum changes in flow and residence time occurred when the minimum n was used for the channel and the maximum n was used for the inset floodplain or vice-a-versa, so only these two cases were analyzed for $F_b = 0.00$, 0.22, 0.44, 0.67, and 1.0. Between these two extremes, RT_{FI} varied by less than 15%, $Q_{F\text{-}FP}$ varied by no more than 50%, and t_{50} within an individual inset floodplain segment varied by no more than 40%. These maximum variations are each less than an order of magnitude, yet the difference in magnitude for residence times and flow between the inset floodplains and structure induced hyporheic zone is several orders of magnitude (Table 4). Additionally, there was no change in the mass stored in the inset floodplains with n. As a result, our conclusions from Table 4 (i.e. Section 4.3 above) would be unaltered by selecting alternative values for n.

ε_t was also varied across a range of reasonable values for natural channels (i.e. 0.01 to 0.2 m^2/s) [*Fischer*, 1973; *Fischer et al.*, 1979], with storm flow models run for $F_b = 0.00$, 0.22, 0.44, 0.67 and 1.0. RT_{FI} varied by a maximum of 35%, and the transport times within individual inset floodplain varied by no more than a factor of 2. There was generally greater variation in transport time with ε_t for the longer inset floodplain segments (higher F_b), due to increased mixing associated with a higher ε_t. There was no change in the mass stored in the inset floodplains or flow through the inset floodplains with ε_t because ε_t is only used for solute transport calculations. The maximum variations are each less than an order of magnitude yet the difference in residence times between floodplains and the structure induced hyporheic zone was several orders of magnitude (Table 4), so the comparison between the two is again unaltered. In addition, both n and ε_t are held constant when evaluating the effect of variations in parameters such as F_b, K, and reach length (e.g., Figures 5, 7-8, 11-12, 14 and 17), so conclusions drawn from the overall trends present in those figures are also independent of these parameters.

2.5. Conclusions

Retention of channel water in off-channel storage zones such as the hyporheic zone or inset floodplains is typically required for significant contaminant reactions to occur in stream systems. We used coupled surface water-groundwater modeling of hydraulics and solute transport (using MIKE-SHE) to analyze the effects of in-stream structures and inset floodplains on solute retention in streams while

varying hydraulic and geologic conditions, and design parameters. In-stream structures induced solute retention in the hyporheic zone at locations where there were relatively neutral groundwater conditions during baseflow. Such hyporheic flow was highly dependent on K. This in-stream structure induced hyporheic flow augments naturally occurring hyporheic flow in streams. Inset floodplain retention occurred only during storm flow when the stream stage was higher than the inset floodplain elevation.

Inset floodplains and in-stream structures retained solutes in dramatically different yet complementary ways (Table 4). For example, in-stream structure induced hyporheic retention occurred for approximately 20% of the year (primarily during summer), while inset floodplains led to surface storage for approximately 1% of the year (during storms). The fraction of stream flow passing through inset floodplains was one to three orders of magnitude higher than that through the in-stream structure induced hyporheic zone, while the residence time in the in-stream structure induced hyporheic zone was approximately three to five orders of magnitude larger than that in the inset floodplains. Further, the solute mass stored in the structure induced hyporheic zone at steady state solute concentrations was approximately 1 order of magnitude larger than that stored in the inset floodplains at steady state solute concentrations. Given these distinctions, neither hyporheic zones nor inset floodplains are expected to simultaneously have both sufficient residence time and sufficient percent of flow to allow substantial contaminant reactions to occur across the majority of their domains. Nevertheless, the spatial heterogeneity of flow rates and residence times within hyporheic or floodplain storage zones means that such conditions should exist at certain locations within these storage zones (hot spots) at certain times (hot moments). To maximize water quality effects, tandem restoration of both feature types is recommended where the stream hydrograph is flashy (favorable for inset floodplain retention), and where sediment hydraulic conductivity is relatively high (favorable for hyporheic retention).

When favorable conditions do exist, simple scaling relationships generated from our model output are useful for understanding the effects of design parameters or constraints (Equations (5-8)). For example, increasing the fraction of the stream bank with inset floodplains increased exchange flow and reach residence times up to a point, after which it leveled off. Increasing the length of restored reach increased hydraulic retention in both structure-induced hyporheic zones and inset floodplains, but may be most important for hyporheic flow because the latter is more limited by exchange rates. Finally, structure-induced hyporheic exchange increased directly with sediment hydraulic conductivity. Results from this study can be used to help make logical design choices with realistic expectations when improving water quality is a primary objective for stream restoration.

2.6. References

Alexander, R. B., R. A. Smith, and G. E. Schwarz (2000), Effect of stream channel size on the delivery of nitrogen to the Gulf of Mexico, *Nature*, *403*(6771), 758-761.

Anderson, M. P., and W. W. Woessner (1992), *Applied Groundwater Modeling : Simulation of Flow and Advective Transport*, Academic Press, San Diego.

Arcement, G. J., and V. R. Schneider (1989), *Guide for Selecting Manning's Roughness Coefficients for Natural Channels and Flood Plains*, v, 38 p. pp., U.S. G.P.O. , Washington, D.C.

Bayley, P. B. (1991), The flood pulse advantage and the restoration of river-floodplain systems, *Regulated Rivers: Research & Management*, *6*(2), 75-86.

BenDor, T., J. Sholtes, and M. W. Doyle (2009), Landscape characteristics of a stream and wetland mitigation banking program, *Ecological applications*, *19*(8), 2078-2092.

Bernhardt, E. S., et al. (2005), Synthesizing U.S. river restoration efforts, *Science*, *308*(5722), 636-637.

Boano, F., C. Camporeale, R. Revelli, and L. Ridolfi (2006), Sinuosity-driven hyporheic exchange in meandering rivers, *Geophysical Research Letters*, *33*(18).

Boulton, A. J., S. Findlay, P. Marmonier, E. H. Stanley, and H. M. Valett (1998), The functional significance of the hyporheic zone in streams and rivers, *Annual Review of Ecology and Systematics*, *29*, 59-81.

Box, J. (1996), Setting objectives and defining outputs for ecological restoration and habitat creation, *Restoration Ecology*, *4*(4), 427-432.

Brunke, M., and T. Gonser (1997), The ecological significance of exchange processes between rivers and groundwater, *Freshwater Biology*, *37*(1), 1-33.

Buchanan, B., M. Walter, G. Nagle, and R. Schneider (2012), Monitoring and assessment of a river restoration project in central New York, *River Research and Applications*, *28*(2), 216-233.

Bukaveckas, P. A. (2007), Effects of channel restoration on water velocity, transient storage, and nutrient uptake in a channelized stream, *Environmental Science & Technology*, *41*(5), 1570-1576.

Calver, A. (2005), Riverbed permeabilities: Information from pooled data, *Ground Water*, *39*(4), 546-553.

Cardenas, M. B., and J. L. Wilson (2006), The influence of ambient groundwater discharge on exchange zones induced by current–bedform interactions, *Journal of Hydrology*, *331*(1), 103-109.

Cardenas, M. B., J. L. Wilson, and V. A. Zlotnik (2004), Impact of heterogeneity, bed forms, and stream curvature on subchannel hyporheic exchange, *Water Resources Research*, *40*(8).

Cerco, C. F., and T. Cole (1993), Three-dimensional eutrophication model of Chesapeake Bay, *Journal of Environmental Engineering*, *119*(6), 1006-1025.

Changxing, S., G. Petts, and A. Gurnell (1999), Bench development along the regulated, lower River Dee, UK, *Earth Surface Processes and Landforms*, *24*(2), 135-149.

Chin, A., S. Anderson, A. Collison, B. J. Ellis-Sugai, J. P. Haltiner, J. B. Hogervorst, G. M. Kondolf, L. S. O'Hirok, A. H. Purcell, and A. L. Riley (2009), Linking theory and practice for restoration of step-pool streams, *Environmental Management*, *43*(4), 645-661.

Cirpka, O. A., and P. K. Kitanidis (2000), An advective-dispersive stream tube approach for the transfer of conservative-tracer data to reactive transport, *Water Resources Research*, *36*(5), 1209-1220, doi: 10.1029/1999WR900355.

Cirpka, O. A., E. O. Frind, and R. Helmig (1999), Numerical simulation of biodegradation controlled by transverse mixing, *Journal of Contaminant Hydrology*, *40*(2), 159-182.

Copeland, C. (2006), Water Quality: Implementing the Clean Water Act *Rep.*, Congressional Research Service Reports. Paper 36.

Craig, L. S., et al. (2008), Stream restoration strategies for reducing river nitrogen loads, *Frontiers in Ecology and the Environment*, *6*(10), 529-538.

Creswell, J. E., S. C. Kerr, M. H. Meyer, C. L. Babiarz, M. M. Shafer, D. E. Armstrong, and E. E. Roden (2008), Factors controlling temporal and spatial distribution of total mercury and methylmercury in hyporheic sediments of the Allequash Creek wetland, northern Wisconsin, *Journal of Geophysical Research: Biogeosciences*, *113*(G2), G00C02, doi: 10.1029/2008JG000742.

Crispell, J. K., and T. A. Endreny (2009), Hyporheic exchange flow around constructed in-channel structures and implications for restoration design, *Hydrological Processes*, *23*(8), 1158-1168, doi: 10.1002/hyp.7230.

Daniluk, T. L., L. K. Lautz, R. P. Gordon, and T. A. Endreny (2012), Surface water–groundwater interaction at restored streams and associated reference reaches, *Hydrological Processes*, doi: 10.1002/hyp.9501.

DHI (Danish Hydraulic Institute) (2011), MIKE SHE User Manual Volume 2: Reference Guide, edited.

Endreny, T., L. Lautz, and D. Siegel (2011a), Hyporheic flow path response to hydraulic jumps at river steps: Flume and hydrodynamic models, *Water Resources Research*, *47*(2), W02517, doi: 10.1029/2009WR008631.

Endreny, T., L. Lautz, and D. Siegel (2011b), Hyporheic flow path response to hydraulic jumps at river steps: Hydrostatic model simulations, *Water Resources Research*, *47*(2), W02518, doi: 10.1029/2010WR010014.

Ensign, S. H., and M. W. Doyle (2005), In-channel transient storage and associated nutrient retention: evidence from experimental manipulations, *Limnology and Oceanography*, *50*(6), 1740-1751.

Filoso, S., and M. A. Palmer (2011), Assessing stream restoration effectiveness at reducing nitrogen export to downstream waters, *Ecological Applications*, *21*(6), 1989-2006.

Fischer, H. B. (1973), Longitudinal dispersion and turbulent mixing in open-channel flow, *Annual Review of Fluid Mechanics*, *5*(1), 59-78.

Fischer, H. B., J. E. List, R. C. Y. Koh, J. Imberger, and N. H. Brooks (1979), *Mixing in Inland and Coastal Waters*, xiv, 483 pp., Academic Press, New York.

FISRWG (Federal Interagency Stream Restoration Working Group) (1998), Stream corridor restoration : principles, processes, and practices *Rep. 0934213593 9780934213592*, Federal Interagency Stream Restoration Working Group, Washington, D.C.

Freeze, R. A., and J. A. Cherry (1979), *Groundwater*, Prentice-Hall, Englewood Cliffs, N.J.

Gelhar, L. W., C. Welty, and K. R. Rehfeldt (1992), A critical review of data on field-scale dispersion in aquifers, *Water Resources Research*, *28*(7), 1955-1974, doi: 10.1029/92WR00607.

Giammarco, P., E. Todini, and P. Lamberti (1996), A conservative finite elements approach to overland flow: the control volume finite element formulation, *Journal of Hydrology*, *175*(1), 267-291.

Graham, D. N., and M. B. Butts (2005), Flexible, integrated watershed modelling with MIKE SHE, *Watershed models*, 245-272.

Haycock, N. E., and T. P. Burt (1993), Role of floodplain sediments in reducing the nitrate concentration of subsurface run-off: A case study in the Cotswolds, UK, *Hydrological Processes*, *7*(3), 287-295, doi: 10.1002/hyp.3360070306.

Heeren, D. M., G. A. Fox, R. B. Miller, D. E. Storm, A. K. Fox, C. J. Penn, T. Halihan, and A. R. Mittelstet (2011), Stage-dependent transient storage of phosphorus in alluvial floodplains, *Hydrological Processes*, *25*(20), 3230-3243, doi: 10.1002/hyp.8054.

Hein, T., C. Baranyi, G. J. Herndl, W. Wanek, and F. Schiemer (2003), Allochthonous and autochthonous particulate organic matter in floodplains of the River Danube: the importance of hydrological connectivity, *Freshwater Biology*, *48*(2), 220-232.

Helton, A. M., G. C. Poole, R. A. Payn, C. Izurieta, and J. A. Stanford (2012), Relative influences of the river channel, floodplain surface, and alluvial aquifer on simulated hydrologic residence time in a montane river floodplain, *Geomorphology, in press*.

Henderson, F. M. (1966), *Open Channel Flow*, xxii, 522 p. pp., Macmillan, New York.

Hester, E. T., and M. W. Doyle (2008), In-stream geomorphic structures as drivers of hyporheic exchange, *Water Resources Research*, *44*(3), W03417, doi: 10.1029/2006WR005810.

Hester, E. T., and M. N. Gooseff (2010), Moving beyond the banks: hyporheic restoration is fundamental to restoring ecological services and functions of streams, *Environmental Science & Technology*, *44*(5), 1521-1525.

Holtz, R. D., and W. D. Kovacs (1981), *An Introduction to Geotechnical Engineering*, Prentice-Hall, Englewood Cliffs, N.J.

Horritt, M., and P. Bates (2001), Predicting floodplain inundation: raster-based modelling versus the finite element approach, *Hydrological Processes*, *15*(5), 825-842, doi: 10.1002/hyp.188.

Hromadka, T., C. Berenbrock, J. Freckleton, and G. Guymon (1985), A two-dimensional dam-break flood plain model, *Advances in Water Resources*, *8*(1), 7-14.

Jin, H.-S., and G. M. Ward (2005), Hydraulic characteristics of a small Coastal Plain stream of the southeastern United States: effects of hydrology and season, *Hydrological Processes*, *19*(20), 4147-4160, doi: 10.1002/hyp.5878.

Kaushal, S. S., P. M. Groffman, P. M. Mayer, E. Striz, and A. J. Gold (2008), Effects of stream restoration on denitrification in an urbanizing watershed, *Ecological Applications*, *18*(3), 789-804.

Kim, H., H. F. Hemond, L. R. Krumholz, and B. A. Cohen (1995), In-situ biodegradation of toluene in a contaminated stream., *Environmental Science & Technology*, *29*(1), 108-116.

Kondolf, G. M., and E. R. Micheli (1995), Evaluating stream restoration projects, *Environmental Management*, *19*(1), 1-15.

Lautz, L. K., and D. l. Siegel (2006), Modeling surface and ground water mixing in the hyporheic zone using MODFLOW and MT3D, *Advances in Water Resources*, *29*(11), 1618-1633.

Leopold, L. B., and M. G. Wolman (1960), River meanders, *Geological Society of America Bulletin*, *71*(6), 769-793.

Mason, S. J. K., B. L. McGlynn, and G. C. Poole (2012), Hydrologic response to channel reconfiguration on Silver Bow Creek, Montana, *Journal of Hydrology (Amsterdam)*, *438*(1), 125-136.

McClain, M. E., E. W. Boyer, C. L. Dent, S. E. Gergel, N. B. Grimm, P. M. Groffman, S. C. Hart, J. W. Harvey, C. A. Johnston, and E. Mayorga (2003), Biogeochemical hot spots and hot moments at the interface of terrestrial and aquatic ecosystems, *Ecosystems*, *6*(4), 301-312.

McCuen, R. (2005), *Hydrologic Analysis and Design*, Pearson Prentice Hall, Englewood Cliffs, NJ.

Menichino, G. T., and E. T. Hester (2013), The effect of hydraulic conductivity and in-stream structures on hyporheic exchange: hydraulics and the hyporheic sweetspot concept., *Water Resources Research, In Review.* .

Menichino, G. T., A. S. Ward, and E. T. Hester (2012), Macropores as preferential flow paths in meander bends, *Hydrological Processes*.

Moussa, R., and C. Bocquillon (2000), Approximation zones of the Saint-Venant equations f flood routing with overbank flow, *Hydrology and Earth System Sciences Discussions*, *4*(2), 251-260.

Nagaoka, H., and S. Ohgaki (1990), Mass transfer mechanism in a porous riverbed, *Water Research*, *24*(4), 417-425.

Naish, C., and R. Sellin (1996), Flow structure in a large-scale model of a doubly meandering compound river channel, *Coherent Flow Structures in Open Channels*, 631-654.

Noe, G. B., and C. R. Hupp (2007), Seasonal variation in nutrient retention during inundation of a short-hydroperiod floodplain, *River Research and Applications*, *23*(10), 1088-1101.

Noe, G. B., C. R. Hupp, and N. B. Rybicki (2013), Hydrogeomorphology influences soil nitrogen and phosphorus mineralization in floodplain wetlands, *Ecosystems*, *16*(1), 75-94.

Opperman, J. J., G. E. Galloway, J. Fargione, J. F. Mount, B. D. Richter, and S. Secchi (2009), Sustainable floodplains through large-scale reconnection to rivers, *Science*, *326*(5959), 1487-1488.

Owens, L. B., W. M. Edwards, and R. W. Keuren (1991), Baseflow and stormflow transport of nutrients from mixed agricultural watersheds, *J. Environ. Qual.*, *20*(2), 407-414.

Pionke, H. B., W. J. Gburek, R. R. Schnabel, A. N. Sharpley, and G. F. Elwinger (1999), Seasonal flow, nutrient concentrations and loading patterns in stream flow draining an agricultural hill-land watershed, *Journal of Hydrology*, *220*(1–2), 62-73.

Rabalais, N. N., R. E. Turner, and D. Scavia (2002), Beyond science into policy: Gulf of Mexico hypoxia and the Mississippi River, *BioScience*, *52*(2), 129-142.

Radspinner, R., P. Diplas, A. F. Lightbody, and F. Sotiropoulos (2010), River training and ecological enhancement potential using in-stream structures, *Journal of Hydraulic Engineering*, *136*(12), 967-980.

Resop, J. P. (2010), Terrestrial Laser Scanning for Quantifying Uncertainty in Fluvial Applications, Ph.D. thesis, Virginia Tech.

Rohde, S., M. Hostmann, A. Peter, and K. C. Ewald (2006), Room for rivers: An integrative search strategy for floodplain restoration, *Landscape and Urban Planning*, *78*(1–2), 50-70.

Roley, S. S., J. L. Tank, and M. A. Williams (2012a), Hydrologic connectivity increases denitrification in the hyporheic zone and restored floodplains of an agricultural stream, *Journal of Geophysical Research*, *117*, G00N04, doi: 10.1029/2012JG001950.

Roley, S. S., J. L. Tank, M. L. Stephen, L. T. Johnson, J. J. Beaulieu, and J. D. Witter (2012b), Floodplain restoration enhances denitrification and reach-scale nitrogen removal in an agricultural stream, *Ecological Applications*, *22*(1), 281-297.

Roni, P., T. J. Beechie, R. E. Bilby, F. E. Leonetti, M. M. Pollock, and G. R. Pess (2002), A review of stream restoration techniques and a hierarchical strategy for prioritizing restoration in pacific northwest watersheds, *North American Journal of Fisheries Management*, *22*(1), 1-20.

Rosgen, D. L. (2001), The Cross-Vane, W-Weir and J-Hook Vane Structures...Their Description, Design and Application for Stream Stabilization and River Restoration, in *Wetlands Engineering & River Restoration 2001*, edited, pp. 1-22, American Society of Civil Engineers.

Royall, D., L. Davis, and D. R. Kimbrow (2010), In-channel benches in small watersheds: examples from the southern piedmont, *Southeastern Geographer*, *50*(4), 445-467.

Royer, T. V., M. B. David, and L. E. Gentry (2006), Timing of riverine export of nitrate and phosphorus from agricultural watersheds in illinois: implications for reducing nutrient loading to the Mississippi River, *Environmental Science & Technology*, *40*(13), 4126-4131.

Salehin, M., A. I. Packman, and M. Paradis (2004), Hyporheic exchange with heterogeneous streambeds: Laboratory experiments and modeling, *Water Resources Research*, *40*(11), W11504, doi: 10.1029/2003WR002567.

Sawyer, A. H., and M. B. Cardenas (2009), Hyporheic flow and residence time distributions in heterogeneous cross-bedded sediment, *Water Resources Research*, *45*(8), W08406, doi: 10.1029/2008WR007632.

Sawyer, A. H., and M. B. Cardenas (2012), Effect of experimental wood addition on hyporheic exchange and thermal dynamics in a losing meadow stream, *Water Resources Research*, *48*(10), W10537, doi: 10.1029/2011WR011776.

Sawyer, A. H., M. B. Cardenas, and J. Buttles (2011), Hyporheic exchange due to channel-spanning logs, *Water Resources Research*, *47*(8), W08502, doi: 10.1029/2011WR010484.

Schnoor, J. L. (1996), *Environmental Modeling: Fate and Transport of Pollutants in Water, Air, and Soil*, John Wiley and Sons.

Schueler, T., and B. Stack (2012), Recommendations of the Expert Panel to Define Removal Rates for Individual Stream Restoration Projects: Final Report *Rep.*, Chesapeak Bay Urban Stormwater Workgroup.

Soar, P. J., and C. R. Thorne (2011), Design discharge for river restoration, *Geophysical Monograph Series*, *194*, 123-149.

Stofleth, J. M., F. D. Shields Jr, and G. A. Fox (2008), Hyporheic and total transient storage in small, sand-bed streams, *Hydrological Processes*, *22*(12), 1885-1894, doi: 10.1002/hyp.6773.

Storey, R. G., K. W. F. Howard, and D. D. Williams (2003), Factors controlling riffle-scale hyporheic exchange flows and their seasonal changes in a gaining stream: A three-dimensional groundwater flow model, *Water Resources Research*, *39*(2), n/a-n/a, doi: 10.1029/2002WR001367.

Thompson, W., C. W. Hession, and D. T. Scott (2012), StREAM Lab at Virginia Tech, *Resources*, *19*(2), 8-9.

Thoms, M. C., and J. M. Olley (2004), The stratigraphy, mode of deposition and age of inset flood plains on the Barwon-Darling River, Australia, *Sediment Transfer Through the Fluvial System*.

Tsai, C. W. (2005), Flood routing in mild-sloped rivers—wave characteristics and downstream backwater effect, *Journal of Hydrology*, *308*(1), 151-167.

USGS (2013), How much water flows during a storm?, edited.

Vest, C. M. (2008), Context and challenge for twenty-first century engineering education, *Journal of Engineering Education*, *97*(3), 235-236.

Ward, A. S., M. Fitzgerald, M. N. Gooseff, T. J. Voltz, A. M. Binley, and K. Singha (2012), Hydrologic and geomorphic controls on hyporheic exchange during base flow recession in a headwater mountain stream, *Water Resources Research, 48*(4), W04513, doi: 10.1029/2011WR011461.

Weill, S., E. Mouche, and J. Patin (2009), A generalized Richards equation for surface/subsurface flow modelling, *Journal of Hydrology*, *366*(1), 9-20.

Wondzell, S. M. (2011), The role of the hyporheic zone across stream networks, *Hydrological Processes, 25*(22), 3525-3532, doi: 10.1002/hyp.8119.

Wondzell, S. M., and F. J. Swanson (1996), Seasonal and storm dynamics of the hyporheic zone of a 4th-order mountain stream. I: Hydrologic processes, *Journal of the North American Benthological Society*, 3-19.

Wood, P. J., and P. D. Armitage (1997), Biological effects of fine sediment in the lotic environment, *Environmental Management*, *21*(2), 203-217.

Wynn, T., C. Hession, and G. Yagow (2010), Stroubles Creek Stream Restoration *Rep.*, Virginia Department of Conservation and Recreation and Virginia Tech Biological Systems Engineering Department.

Zarnetske, J. P., R. Haggerty, S. M. Wondzell, and M. A. Baker (2011), Dynamics of nitrate production and removal as a function of residence time in the hyporheic zone, *Journal of Geophysical Research*, *116*(G1), G01025.

Zarnetske, J. P., R. Haggerty, S. M. Wondzell, V. A. Bokil, and R. González-Pinzón (2012), Coupled transport and reaction kinetics control the nitrate source-sink function of hyporheic zones, *Water Resources Research, 48*(11), W11508, doi: 10.1029/2012WR011894.

3. Engineering Applications

The relationship between stream restoration and stream water quality is complicated, largely because the relationship between solute retention and stream restoration is complex. The goal of this study was to assist stream restoration practitioners and designers in making stream restoration design decisions when improving water quality is a goal. Since retention of channel water in off-channel storage zones such as the hyporheic zone or inset floodplains is typically required for significant contaminant reactions to occur in stream systems, this was the focus of the study. We used coupled surface water-groundwater modeling of hydraulics and solute transport (using MIKE-SHE) to analyze the effects of channel spanning in-stream structures and inset floodplains on solute retention in streams while varying hydraulic and geologic conditions. The complementarity of different stream restoration techniques has not been studied extensively up to this point, and this study offers such a rigorous analysis for in-stream structures and inset floodplains.

Solute retention occurred in the in-stream structure induced hyporheic zone and in inset floodplains for drastically different yet complementary hydraulic conditions (Table 4). In-stream structure induced solute retention occurred in the hyporheic zone when there were relatively neutral groundwater conditions during baseflow~~, and where the hydraulic conductivity was sufficiently large for a substantial amount of flow to move through the hyporheic zone~~. This in-stream structure induced hyporheic flow augments naturally occurring hyporheic flow in streams. Inset floodplain retention occurred only during storm flow when the stream stage was higher than the inset floodplain elevation. To retain solutes for both storm flow conditions and summer baseflow conditions at Stroubles Creek both stream restoration techniques were necessary. For this study the hydraulic conditions necessary to induce in-stream structure induced hyporheic flow occurred for approximately 20% of the year, and the stream stage required for inset floodplain retention occurred for approximately 1% of the year. These values will vary from one stream to another, but the necessity of utilizing both restoration practices together to retain solutes during both storm flow and baseflow conditions is an important conclusion.

The fraction of stream flow passing through inset floodplains was one to three orders of magnitude higher than that through the in-stream structure induced hyporheic zone, while the residence time in the in-stream structure induced hyporheic zone was approximately three to five orders of magnitude larger than that in the inset floodplains. Further, the solute mass stored in the structure induced hyporheic zone at steady state solute concentrations was approximately 1 order of magnitude larger than that stored in the inset floodplains at steady state solute concentrations. Given these distinctions, for a 90 m restoration reach neither in-stream structure induced hyporheic zones nor inset floodplains ~~are~~ were expected to simultaneously have both sufficient residence time and sufficient percent of flow to allow substantial pollutant reactions to occur across the majority of their domains.

Nevertheless, the spatial heterogeneity of flow rates and residence times within hyporheic or floodplain storage zones means that such conditions should exist at certain locations within these storage zones (hot spots) at certain times (hot moments). To maximize water quality effects when pollutant loading is occurring for both baseflow and storm flow conditions, tandem restoration of both feature types is recommended where the stream hydrograph is flashy (favorable for inset floodplain retention), and where sediment hydraulic conductivity is relatively high (favorable for hyporheic retention).

Scaling equations were generated to estimate storage in inset floodplains and in-stream structure induced hyporheic zones as function of length of restored reach and other design parameters. The fraction of channel flow that entered the structure induced hyporheic zone at Stroubles Creek can be calculated using Equation (5) based on the hydraulic conductivity and the length of reach restored. Equation (6) generalized Equation (5) to take into account the effects of the structure density and the hydraulics of the system. From this relationship it appeared that a significant fraction of flow cannot enter the hyporheic zone if the hydraulic gradient across the structure approaches zero (e.g., the system is highly gaining or losing) or if the hydraulic conductivity is low. This is a key insight for practitioners, as hyporheic storage is highly dependent on both the system hydraulics and the geology. Water quality improvement estimates for a stream where either of these variables is unknown is therefore highly uncertain. The hydraulic conditions and geology vary spatially and the hydraulic conditions also vary temporally, so hydraulic and geologic measurements at multiple locations along a stream reach are necessary to understand the potential for water quality effects. The relationship between the fraction of bank with inset floodplain and the reach residence time is described by Equation (7) and Equation (8). The reach residence times increased as the bank fraction increased, until leveling off at a bank fraction of 0.67. This relationship indicates that restoring a longer reach with a bank fraction less than 1 may lead to more retention than installing a full inset floodplain over a shorter reach (assuming the total length of restored bank is the same).

This study is primarily focused on solute retention and not reactant availability; however, general pollutant loading trends (or ideally data at stream restoration locations) are necessary for estimating actual water quality improvements. For example, phosphorous and sediment loading primarily occurs during storm flow conditions. If decreasing the concentrations of either of these is the primary goal of a stream restoration project then practices that focus on storm flow hydraulic conditions (e.g., inset floodplains) will be most effective. Practices that only retain solutes during baseflow hydraulic conditions (including in-stream structures) will be less effective in reducing phosphorous or sediment loading. Nitrate removal processes tend to occur more evenly over the year, so depending on the site specific loading rates stream restoration techniques that focus on baseflow (e.g., in-stream structures) and storm flow (e.g., inset floodplains) may be useful in tandem. Stream restoration designers should understand when retention is

occurring for various restoration practices, what loading is most likely to occur at those times, and whether the solute retention is sufficient for nutrient removal. Only with this fundamental understanding of solute retention induced by the various stream restoration practices will the potential for water quality improvement be recognized. Results from this study can be used to help make logical design choices with realistic expectations when improving water quality is an objective for stream restoration projects.

Appendix A: Detailed Description of Modeling Methodology

A.1. Background

This appendix supplements the information from Section 2.2. to aid future researchers in using MIKE SHE for hydraulic and solute transport modeling. This is a combination of generalized and interpretive modeling study, with physical parameters based on Stroubles Creek, but generalized enough (e.g., omitting micro topography, a clay lens, and intrusive bedrock) to be useful when considering any small agricultural or urban stream. All assumptions made in this study were made with the understanding that this is a mix of a generalized and interpretive study.

MIKE SHE is an integrated hydraulic and hydrologic model that has tools to model groundwater flow, two dimensional surface water flow (overland flow), one dimensional channel flow, precipitation, evaporation, flow through the unsaturated zone, as well as several other processes. For this research the three dimensional groundwater flow component and the two dimensional surface water flow components were used. Solute transport can be modeled using the advection dispersion equation between different components. There are various limitations to this solute transport, such as the inability of solute to leave the one dimensional channels after entering them. Solute can be exchanged from the saturated zone to and from the two dimensional surface water flow however, which is why the two dimensional surface water flow tool was used instead of the one dimensional channel tool for this study.

The overall methodology used for running models in this study will be discussed (A.2.), as well as specific details on model inputs (A.3.). The modeling methodology includes the strategy for both hydraulic and water quality (solute transport) modeling. Model grid inputs (e.g., saturated zone geometry, topography, boundary conditions) were too large to include in this thesis (7,850 cells). MIKE SHE uses unique file types for all data files: dsf0 for 1 dimensional time series, dsf2 for grid data, and dfs3 for grid data that varies with time.

A.2. Overall Modeling Strategy

A.2.1. Hydraulic Modeling

The hydraulic models ("Water Management" in MIKE SHE) were run first for each model scenario followed by the solute transport ("Water Quality" in MIKE SHE). For the hydraulic modeling the surface water component was much more numerically demanding than the groundwater component, and as a result took much longer to run for the same modeled time period. For example, modeling 1 hour (model time) would take less than ten seconds to run for the groundwater component, and between 15 minutes and 2 hours for the surface water component (depending on the hydraulic conditions and the inset floodplain length). The groundwater required a long model period to reach steady state (e.g., over a week model time) but ran quickly while the surface water reached steady state quickly (~1 hour model time)

but ran slowly. For reasonable model run times the groundwater and surface water components were initially run independently, before being run together. The method used to do this was as follows:

1. The groundwater was run to steady state assuming the stream channel was dry, for both the summer and winter baseflow groundwater conditions.
2. The results from step 1 were used as initial groundwater conditions (for each of the 25 layers) for a combined surface water groundwater model with the correct boundary conditions until steady state was reached in the surface water (~1 hour model time).
    a. At this point the upstream and downstream surface water boundary conditions were edited as needed to have the desired stream flow (see 2.2.2.6.).
    b. This is not enough time for the groundwater component to reach steady state.
3. The surface water elevations from step 2 were input as fixed head boundaries for a groundwater model (without surface water modeled), and the model was run to steady state.
4. The results from step 3 were used as initial groundwater conditions (for each of the 25 layers) and run together with the surface water modeling component. With the groundwater and surface water levels relatively close to their coupled values it took less than 12 hours (model time) to reach a steady state condition.

This methodology was used with data stored every hour for the groundwater and surface water components, although actual time steps were much smaller ("large" storing intervals were due to the size of data files). The storm flow scenario was run with the summer baseflow steady state groundwater conditions, since storms generally last less than 12 hours.

A.2.2. Solute Transport Modeling

Solute transport modeling using MIKE SHE required short time steps to yield smooth breakthrough tracer curves, so each of the hydraulic model scenarios were re-run with smaller storage intervals. MIKE SHE can save "hot-start" data which allows a model to be run starting from the end of a previous model run. This allowed for an additional 2 hours (model time) to run for each scenario starting from the end of the hydraulic models (discussed in A.2.1.). Data was stored every 0.1 hours for groundwater component, and every 0.01 hours for the surface water component. The water quality output was 0.001 hours for the surface water component and 6 hours for the groundwater component based on smoothness of breakthrough tracer curves and the time to reach steady state tracer concentrations. Tracer was added to the northernmost channel cells (at the top row) of the model domain. The tracer input was optimized so that the concentration in each of these cells was 1 g/m^3 with each of the cells requiring a different tracer input. The tracer input was typically optimized after 5 to 20 iterations.

A.2.3. Post Processing

Once the final hydraulic and solute transport models were run, post processing was done using a mix of basic MIKE SHE output and extracted results using the MIKE Zero Toolbox. Additional data computation was done using Microsoft Excel (including visual basic macro's). Flow depth, solute mass, groundwater head elevations, groundwater flow, and exchange flow (groundwater to surface water) are all available as grid data from the MIKE SHE output. Breakthrough tracer curves had to be extracted using the MIKE Zero Toolbox "Time series from 2D Data" and "Time Series from 3D Data" tools.

A.3. Detailed Description of Model Inputs

A.3.1. Simulation Specifications

A.3.1.1. Simulation Period

Depending on the model run, either both the Saturated Zone Flow (SZ, groundwater) model and the Overland Flow (OL, surface water) models were run, or only the groundwater component. For all model runs the start date was 1/1/2000 12:00 AM, with the models run for 2 to 12 hours model time (run to between 2:00 AM and 12:00 PM) depending on what models from A.2. were being run.

A.3.1.2. Time Step Control

The maximum time step controls were set to 0.001 hours for the surface water component, and 0.01 hours for the groundwater. Recommended values were used for all other time step control parameters.

A.3.1.3. Overland Flow (Surface Water) Computational Control Parameters

The "Explicit" surface water solver was used instead of the "Successive Overrelaxation" due to stability issues and model run times. A courant number of 0.8 was used, with threshold water depths of 0.001 and threshold gradients for applying low-gradient floe reduction of 0.001.

A.3.1.4. Saturated Zone (groundwater) Computational Control Parameters

The "Preconditioned Conjugate Gradient, Transient" solver was used for groundwater flow when both surface water and groundwater were modeled, while the "Preconditioned Conjugate Gradient, Steady State" solver was used when only groundwater flow was modeled. The recommended values were used for all iteration control and advanced settings for the groundwater computational control.

A.3.2. Model Domain and Grid

A domain shapefile was created in ArcGIS and was used to create the model domain. The number of cells in the X and Y directions were set to 110, and the cells size was set to 1 m (MIKE SHE uses a square grid so this corresponds to 1 m^2). The domain was rotated to line up with the channel (16°) and the catchment origin was selected so the entire model domain was included in the catchment.

A.3.3. Topography

As discussed in 2.2.2.3., the topography input for MIKE SHE was created by overlaying surveyed stream cross sections over existing topography data. This was done using the process below:

1. A separate MIKE SHE file was created that was solely used to construct the "topography" inputs.
    a. This file used a grid file created from LIDAR data in GIS as the base topography.
    b. The Rivers and Lakes (OC) engine was enabled, allowing MIKE SHE to run with MIKE 11 (a one dimensional channel model similar to HEC-RAS).
2. A MIKE 11 file was created and cross sections were imported.
    a. A stream centerline shapefile was created in ArcGIS and imported to MIKE 11.
    b. Cross sections could be created as needed along the stream center line (station and elevation are given at various cross sections) to construct the desired topography.
    c. The longitudinal slope was based on a longitudinal survey that occurred after the restoration occurred (StREAM Lab), and was tied into the existing topography based on the cross sections surveyed for this study.
3. The MIKE SHE Topography file was run with "grid codes" selected in the Rivers and Lakes tab, allowing for the MIKE 11 cross sections to superimpose over existing topography (effectively overlaying the grid file).
4. The MIKE SHE pre-processor was run, and the topography (with the channel superimposed) could be viewed, copied, and saved to be used for other MIKE SHE models (without MIKE 11).

The inset floodplain segments were centered at the apex of the 4 northernmost meanders in the model domain, and were 0, 10, 20, and 30 m long. A full inset floodplain was also created. The dfs2 grid file output from this process could simply be selected as the topography file in MIKE SHE. The structures were added by setting the topography to 30 cm above the thalweg at the structure locations, and setting the elevations to all adjacent cells (perpendicular to channel flow) to that elevation until the natural topography was at a higher elevation.

A.3.4. Overland Flow (Two Dimensional Surface Water)

The Manning's n was higher in the inset floodplain than it was in the main channel so the Manning's n was represented by a grid file (dfs2). The inset floodplain delineation was based on the depth of water during storm flow (shallower depth over inset floodplain) using excel, and then was exported to a dfs2 file. The detention storage, initial water depth, initial mass, and the dispersion coefficient along rows were all uniformly set to 0 for the entire domain. The dispersion coefficient along columns (the transverse direction) was set uniformly to 0.04 m^2/s for the entire domain.

A.3.5. Saturated Zone

A.3.5.1. Geological Layers

There were two geological layers used in this study: a floodplain/bank clay loam and a stream bed/ aquifer silty-gravel. MIKE SHE does not allow a layer to have a thickness of 0 when multiple geological layers are present, which occurred at the stream bed where only the silty-gravel was present. To compensate for this the clay loam was set as the geological layer for the entire domain, and a silty-gravel lens was added (see A.3.5.2.). Since a lens is superimposed over whatever geological layers are present, MIKE SHE accepted having no clay loam area directly underneath the stream. The upper level of the layer was set uniformly to 0 m with the "relative to ground" box checked. The lower level was calculated using the topography grid and Excel. The minimum elevation was calculated for each row (which occurred at the thalweg), and the lower domain was set 5 m below this elevation for each row. This resulted in a consistent elevation for the lower domain along a row, and a decrease in the elevation corresponding with the longitudinal slope when moving along a column. The hydraulic conductivity, specific yield, specific storage, porosity, longitudinal dispersivity, and transverse dispersivity were set as uniform for the entire model domain (see Table 1 for values).

A.3.5.2. Geological Lenses

Two layers were modeled as lenses for this thesis: the silty-gravel representing the stream sediment and aquifer, and a highly impermeable layer representing the structures. The horizontal extent of the silty-gravel layer was the entire model domain. From StREAM Lab soil borings the silty-gravel begins approximately 30 cm above the channel bottom and this elevation is assumed constant moving laterally away from the stream. The upper level of this lens is then calculated in excel by adding 5.3 m to the lower domain elevation (see A.3.5.1. for description of calculating lower domain elevation). The lower domain is set as the lower domain calculated from A.3.5.1., so the clay loam rests over the silty-gravel layer where clay loam is present (only the silty-gravel is present directly under the stream bed).

The hydraulic conductivity, specific yield, specific storage, porosity, longitudinal dispersivity, and transverse dispersivity were uniform values for the entire model domain (see Table 1 for values).

The geological lens representing the in-stream structures had a horizontal extent that only included the cells where the in-stream structures were present (5 cells). The upper level of the layer was set uniformly as 0 m with the "relative to ground" box checked (only the locations specified by the horizontal extent are read). The lower extent is set as the elevation at the bottom of the upper model layer (the methodology of creating this grid is discussed in A.3.5.3.) which was about 0.2 m below the ground surface. The hydraulic conductivity was set to 1×10^{-15} m/s, the specific yield was set to 0.2, the storage coefficient was set to 0.0001 m^{-1}, the porosity was set to 0.2, and the dispersivities were set to 0 m. These parameters created structures that were effectively impervious.

A.3.5.3. Computational Layers

A different computational layer was required for each of the 25 vertical model layers, each requiring a lower level, initial head, and outer boundary conditions. Fixed head boundary conditions were calculated based on the piezometer data (as discussed in 2.2.2.6.) and were identical for all layers. Excel was used to calculate the lower level of the computation model layers. For each horizontal grid cell location (at a location in x and y) the distance from the ground surface to the bottom of the model domain was calculated. The lower elevation of each layer was calculated by dividing the total model depth for each horizontal location by the 25 model layers, and subtracting this distance consecutively from one computation layer to the next. Each computational grid had a sheet in excel, and had to be copied into a MIKE SHE dfs2 file. The initial head for each layer is copied from the groundwater model results (A.2.1.) into an initial head dfs2 file. This process was completed one at a time for each computation layer, with the correct item specified for each file (e.g., for the top layer you would want to select the first item in the dfs2 file that had all 25 layers in it). This process could be time intensive, and care was taken not to make mistakes when copying and pasting grids.

A.3.6. Water Quality Simulation Specifications

The water quality simulation specifications (the solute transport specifications) must be set for all model runs, even when solute transport is not run (A.2.2.). The data required for water quality modeling is only saved if this done, so that if the model is used as a starting point ("hot start") for a solute transport model the data is there. The water quality must be selected for the Overland Flow (OL) and for the Saturated Zone Flow (SZ). The start date was set to 2000/01/01 1:00 for all solute transport model runs, and the end date was set to 2000/01/01 2:00 when no hyporheic flow was occurring, and 2002/01/01 1:00 for models where hyporheic flow was occurring. No recycling of flow results was specified for the

former, while recycling of flow results was specified for the later (from 2000/01/01 1:00 to 2000/01/01 2:00). The default water quality time step controls were used for this study.

A.3.7.Water Quality Sources

The water quality source (solute transport source) used for this study was located in the "surface", and the source type was "overland". This meant that the solute was being added directly to the surface water. For convenience the "horizontal extent" was the entire model domain, but an integer grid file was created that specified 6 different grid codes (each cell in the domain was given an integer number). Grid codes 1 – 5 were set to the single cells at the upstream boundary within the model domain that were inundated with the storm flow surface water boundary conditions (i.e. 0.65 m). The final grid code was 11, and signified all other cells in the model domain. The solute tracer loading could be adjusted for each grid code, and was optimized until the concentration of each inundated cell was 1 g/m^3 (see A.2.2.). Either a constant or time varying tracer input (g/day) could be used. For models that did not focus on the hyporheic zone the loading was turned off after 10 minutes so a time varying dfs0 file was used to indicate the tracer loading. These files simply had columns representing the loading rate for each that varied with time.

A.3.8. Storing of Results

As discussed in A.2. the storing of results varied from initial hydraulic model runs to the final hydraulic/solute transport models. The initial hydraulic models stored surface water and groundwater data every hour, while the final solute transport model runs stored surface water data every 0.01 hours, and groundwater data every 0.1 hours. The smaller storing intervals led to more stable solute transport models, although the output files were substantially larger. The actual time steps were generally much smaller than the stored time steps. The solute transport data was stored every 0.001 hours for the solute in surface water, and every 6 hours for the solute in groundwater. The reason for this difference had to do with the smoothness of the breakthrough tracer curves and the size of the data files. Since the hyporheic flow reached steady state slowly, huge files would be created if the storing intervals were smaller.

A.3.9. Extra Parameters

To set a specified stage boundary condition for the two dimensional surface water flow (overland flow) the "time varying overland flow boundary" extra parameter was used. This allowed an upstream and downstream stage to be set at the boundary from a dfs2 grid file that could be changed easily from one model run to the next. For a detailed description of how the extra parameters function (and the "time varying overland flow boundary" in particular) it is recommended to look at the MIKE SHE user manual.

The inputs for this parameter are (1) a binary grid file signifying what boundary cells have water and (2) a grid file with the boundary stream stage elevation. In addition, since dfs2 grid files can have several different grids in the same file, the item number must be specified for each of the input files. Both the integer and stream stage grids varied for the different hydraulic conditions (summer baseflow, winter baseflow, and storm flow).

A.3.10. Additional Features Not Used in Thesis

Various components of MIKE SHE were omitted for this study. The modeling components omitted include the Rivers and Lakes (one dimensional surface water flow similar to HEC-RAS), the Unsaturated Zone Modeling (using the full Richardson equation), and Evapotranspiration. Lastly for the groundwater and two dimensional surface water components the climate and landuse could have been specified, but were omitted.